Green Synthesis and Characterization of Zinc Oxide Nanoparticles and their Application as an Optoelectronic Humidity Sensor

Dissertation in partial fulfilment of the requirements for the degree of

MASTER OF TECHNOLOGY

in

NANO-OPTOELECTRONICS

by

CHANDRA MOHINI
B.Tech – ECE

Under the Supervision

of

Prof B. C. Yadav

Department of Electronics and Communication Engineering
University Institute of Engineering and Technology
BABASAHEB BHIMRAO AMBEDKAR UNIVERSITY
(A Central University)
Lucknow-226025, Uttar Pradesh, India

CERTIFICATE

This is to certify that **Miss Chandra Mohini** has worked under our guidance and the report submitted in the project entitle **"Green Synthesis and Characterization of Zinc Oxide Nanoparticles and their Application as an Opto-electronic Humidity Sensor"** is suitable for the award of the degree of Master of Technology.

B Yadav 05/07/2018

(Prof. B. C. Yadav)

Thesis Supervisor, Coordinator, M.Tech (Nano-optoelectronics), University Institute of Engineering and Technology
Babasaheb Bhimrao Ambedkar University, Lucknow

(Prof. Kaman Singh)

Director
University Institute of Engineering and Technology
Babasaheb Bhimrao Ambedkar University, Lucknow

DECLARATION

I hereby declare that this project report entitled **"Green Synthesis and Characterization of Zinc Oxide Nanoparticles and their Application as an Opto-electronic Humidity Sensor"** is an authentic work carried out by me during the session 2016-18, under the supervision of **Prof. B. C. Yadav**, University Institute of Engineering and Technology, Babasaheb Bhimrao Ambedkar University, Lucknow, Uttar Pradesh, India. This dissertation is submitted for the partial fulfilment of the requirement for the award of the degree of Master of Technology in Nano-Optoelectronics.

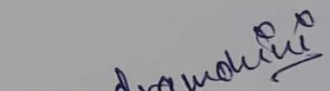

(CHANDRA MOHINI)

M.Tech (Nano-Optoelectronics)
4TH Semester, Roll No. 116035
UIET, Babasaheb Bhimrao Ambedkar University
Lucknow-226025, Uttar Pradesh, India

Dedicated to My Parents

ACKNOWLEDGEMENT

I consider it my greatest privilege to have worked under the guidance of **Prof. Bal Chandra Yadav,** Co-ordinator, M.Tech. (Nano-Optoelectronics Program). I hereby express my deep sense of gratitude and indebtedness to him for his scholastic guidance, ceaseless encouragement, innovative ideas, suggestions, critical evaluations, the incessant devotion of time at every stage of the entire course of my study and preparing this dissertation.

It is very pleasant for me to avail the opportunity to convey my heartfelt thanks to **Prof. Kaman Singh,** Director, University Institute of Engineering and Technology, Babasaheb Bhimrao Ambedkar University Lucknow for his invaluable suggestions and constant encouragements.

I deem it a unique opportunity and utmost pride to express my profound sense of gratitude to **Dr. Richa Srivastava** from whom I learned the methods for doing science and Technology. Also, I am thankful to the reviewers of the dissertation, **Er. Ekta Singh** for valuable suggestions to improve the work and fruitful discussions.

I acknowledge **Ms Samiksha Sikarwar**, Department of Physics, and I am very thankful to **Mr. Ashok Kumar,** research scholar Department of Chemistry, BBAU.

It was the love, blessings, and encouragements of my Parents **Mr. Shoveer Singh** and **Mrs. Vimla Devi** , my brothers **Er. Karuna S. B .**and **Er. Ganesh S. B**., my sisters **Mrs. Hina B.** and **Er. Chitra B.** which made it possible for me to complete this work and pursue my educational career.

Last but not the least; I would like to thank the **God** Almighty, for his blessings without which I wouldn't have been successful in life.

Date: 28th May, 2018

Place: LUCKNOW

CHANDRA MOHINI

M.Tech (Nano-Optoelectronics)

PREFACE

The design of experiments, data analysis and writing of this thesis was done under the supervision of **Prof. B. C. Yadav**. Excluding the following data collection steps, all the other data collection and analysis were performed by the author.

- Department of Horticulture, BBAU.
- SEM, EDX and FTIR data were taken from USIC, BBAU.
- UV-Vis data was collected from Nanomaterials & Sensors Research Laboratory, Department of Physics, BBAU.
- XRD data were collected from the Department of ACMS, IIT Kanpur.
- BET & ZPC data were collected from the Department of Chemistry, BBAU.
- The Opto-Electronic Humidity Sensing application data was observed under the guidance of Professor B.C. Yadav.

ABSTRACT

In this present work, zinc oxide nanoparticles were successfully synthesized by chemical precipitation method. ZnO is a highly demanding material for Opto-electronic devices as it has a wide direct band gap ~ 3.37 eV at room temperature and the high exciton binding energy i.e. 60 meV which makes it capable for excitonic emission at room temperature (RT) and ultraviolet (UV) luminescence at room temperature. The sample was characterized by XRD, SEM, EDX, FTIR, and BET. The optical properties of the sample were investigated through UV-Vis absorption spectra at room temperature. Further, the prepared film was investigated through the exposure of humidity at room temperature and relative humidity (%RH) was measured directly in terms of modulation in the intensity of light recorded on a digital power meter. Synthesis process of ZnO was easy and eco-friendly. Being opto-electronic in nature it can also be employed for remote sensing applications for humidity measurements.

LIST OF CONTENTS

LIST OF FIGURES

LIST OF TABLES

CHAPTER

1

1. INTRODUCTION

1.1 Nanotechnology

Nanotechnology is the science and technology of nanoscale things. The term nanotechnology is the combination of two words: Nano and Technology, the word nano are taken from the Greek numerical prefix nano. Nanotechnology is generally considered in the range of 1 nm to 100 nm or 0.001 μm to 0.1 μm. 1nm equals to 10^{-9}m, in comparison to human hair is about 60,000 to 80,000 nm wide. Nanoscience studies the phenomenon, properties and principle of the material at the nanoscale range, while Nanotechnology deals with design, characterization, production and different applications of the material, by controlling the size and shape [1,2].

Nanotechnology is breaking down long-standing edges between scientific fields, for example, biology has commonly been distinguished by the required attributes of biology organism to replicate, emerge in response in their environment and communicate with another organic system such as those within the human body. As nanotechnology moves closer to the assembly of nano-machines that can multiply respond to their biosphere, communicate with living tissues, and work complicated computing functions, then many of the boundaries between physics, engineering, biology, genetics, medicines, material science, machine science and information technology be blend even further [3]. Most of the early uses of nanotechnology involve relatively simple nanomaterials-such as powders, coating, and introductory elements. Nanomaterials will likely be made thinner, more uniform, selective and reflective of specific illumination frequencies, microbe repellent, strain blocking, water repellent, abrasion resistant, fire resistant, highly insulating and superconductive. These attributes have led to coating and matter for sunscreen, cosmetics, paint, hospital equipment surfaces, clothing fabrics, lubricating surfaces, battery elements, electronics wiring and wire coverings [3].

Nanocrystals are formed when atoms clusters in an orderly configuration with some degree of guidance from microenvironmental conditions. There is variation in the degree they autonomously “self-assembled” and the degree to which their formation is directed by the specifics design of biosphere. The principle additionally applies to the creation of nanocrystalline structures such as nanotubes, nanospheres, and nanowires. for example, nanotubes are grown by subjecting extremely hot carbon material to an intense electrical charge[3].

Nonmanufacturing is the assembly of composite commodities with atomic or nanoscopic stage refinement, in theory, a nanofactory can build anything one atom at a time. However, the present manufacturing process generally involves the construction and assembly of nanocrystalline structures such as nanotubes and nanoshells into materials and goods, instead of assembling unique atoms or molecules one at a time [3].

Nanotechnology helps to solve the serious human problems like energy capability, climate change or fatal diseases. Nanotechnology does not only boost the industry but also create new products that will make positive changes in the lives of citizens, be it in medicine, environment, electronics and other fields. Nanotechnologies and Nanoscience open a new avenue of research, useful and unexpected applications. Novel and newly developed material surface allow giving better performance. Computers are developing by using nanoscale components and also improving their performance which depends on reducing the dimensions [1].

Nanomaterials have unique properties like CNT, Fullerenes, quantum dots, quantum wires, nanofibers and also nanocomposites which give new applications in different fields. It shows unique properties due to their small size and large surface area. According to ref. [2] the surface area to volume ratio for the same material with radius 1 mm, 1 μm, and 1 nm, is obviously different. The increase is more than millionfold in the surface to volume ratio realized when particle converted from millimetre to nanometer. Now a day's commercial products are available like metals, ceramics, polymers, smart textile, cosmetics, sunscreens, electronics, paints and more [1].

However new methods and instruments are developed to increase the knowledge and information of their properties. Nanomaterials must be examined to potential effects of material on health to take precaution and their impacts on the environment [1].

Use of Nanotechnology

- Industries
- Medical Sciences
- Computer Field
- Other uses :
    - Nanofoster material
    - Water purification, etc.

1.2 PROPERTIES OF NANOMATERIALS

Nanostructure materials are single phase and multiphase polycrystalline solids with signify size in nanometres. Here dimension became equivalent with a wavelength of photons. The changes in different properties of the material are like- electronic, mechanical, thermal, optical, electrical etc. for small sized material, the surface to volume ratio take an important task and most of the molecules make the material-energetic by interaction on the surface. Due to quantum mechanics effect, the motion of the erratically moving electrons gets confined to specific energy levels. It affects the electrical magnetic and optical properties of nanoparticles. Due to this effect, the thermal conductivity of nanomaterials decreases. The thermal conductivity decreases by the factors of five in the nano range.

Nanomaterials in dissimilar forms

- Quantum dot
- Nanoparticles
- Nano-clusters
- Nano well and Nanowire
- Bulk nanostructured material
- Carbon nanostructures
- Superfluid clusters
- Magnetic clusters
- Nanostructured ferromagnetism, etc.

Nano- Devices

- Atomic switches
- NEM_S
- Molecular machine
- Nanorobots
- Single electron transistors
- Drug delivery systems
- Nano biometrics

1.3 OPTICAL PHENOMENON

Based on the material, optical phenomena occur due to the interaction of light or matter. As the light in the shape of EM wave and the wave can be detected by Maxwell equations. Optical phenomenon carries optical properties, therefore the law of reflection and refraction offer very good clarification for it. They are many types of optical phenomena like- wave optics, Ray optics, Fourier optics, quantum optics and geometrical optics. In the case of wave optics, which consist of the wave nature of light, such as interaction, diffraction, and polarization.

Ray optics behaves towards the straight line that bent and reflected at angle followed by Snell's law:

- Electro-Opto Effect
- Thermal emission
- Photoemissivity
- Photoelectric Effect
- Luminescence

Luminescence is further categorized into following types:

- Photoluminescence
- Fluorescence
- Phosphorescence
- Cathode-luminescence
- Electro-luminescence

1.4 OPTOELECTRONICS

Optoelectronics is the branch of electronics overlies with Physics. The field concerns the theory, operation, design, and manufacturing that convert the electrical signal to visible or infrared radiation energy or vice versa. Example of optoelectronic components includes LED,

OLED, Laser, optodetector, optocoupler, optical fibre communication solar cell and photocells etc.

Optoelectronics devices are those devices whose function involves the interaction of photons with semiconductors. According to their application, the devices are listed below:

- LED/OLED (Non- coherent sources)
- Laser (coherent sources)
- Photodiodes
- Solar cells
- Opto-isolators
- Optical fibre etc.

This is the study of electronic devices in various fields. It interacts with light and usually, it considered a subfield of photonics. The light often gives invisible radiation such as Gamma rays, UV and Infrared. These devices are a transducer, which converts electrical to optical or optical to electrical is used in devices for their operations.

III-V group element is semiconductors (SCs) which played important role in the development of optoelectronics devices (OED) for different applications such as optical fibre communications, infrared, visible light emitting diodes or laser diodes, solar cells and many more. Semiconductor devices have become an integral part of our lives. OEDs involve interaction between electrons and photons. Direct bandgap SCs show good absorption and emission characteristics which are best for such applications. The elements of group III and V of the periodic table are mostly used for the OED. These SC materials are finding different applications based on their parameters. The band gap of SC material can be engineered by alloying them. Band gap engineering is the formation of heterojunction that is critical for the design of high-performance OEDs such as Lasers [4].

Materials based on small molecules exhibit well-defined optical and electrical properties, making them ideal active components in optoelectronic devices such as LEDs, FETs, and solar cells. These basic devices can be used to develop flexible displays, smart windows, sensors, memories, etc. with the promise of low-cost manufacturing [4]. However, it is infamous that these materials possess nanoscale heterogeneities in their optical and electrical properties that affect

the device performances. These heterogeneities arise from structural and morphological features that vary as a function of the type of chosen molecule and substrate, film processing and device fabrication conditions[5]. Structural factors such as amorphous regions, grain boundaries, and local defects within crystalline domains or phase segregated blends have been shown to directly correlate with the optoelectronic properties of these organic materials and more specifically with charge carrier mobility in field-effect transistors or efficiency in solar cells [6-8]. The characterization of these structural defects, which are responsible for lowering of the performance, is, therefore, an important goal of organic optoelectronics. Characterization techniques based on light-matter interactions, ranging from optical spectroscopy to X-ray based techniques, have been largely used to correlate the structure of organic materials to their charge transport characteristics, and are being constantly improved in terms of spatial and energetic resolution. However, the smallest area that is probed in a single measurement done with these techniques amounts to some mm [2], thus the obtained signals are averaged out of an Avogadro number of molecules. Scanning probe microscopy (SPM) offers unrivalled insights into these issues by providing a high-resolution direct view of the thin films morphology, size and orientation of crystalline domains or grain boundaries on the nanometer scale. The former provides a direct access to the intrinsic electrical properties at the nanoscale by measuring the current flowing between the tip and the conductive sample. The latter makes it possible to monitor the electrical potential even in working devices. Even electric perturbation of the sample is minimal because the instrument tries to match the potential of the tip with one of the sample, thus minimizing any electrostatic interaction between the two.

Self-assembled monolayers (SAMs) on solid surfaces are the key since they enable the tuning of the energetic electrodes at the interfaces, and are also important model systems for investigating the conduction mechanisms along single molecules. Then, come to the SPM which can be used to map the morphology of thin films and to detect the electrical properties of high performing organic semiconducting materials integrated Organic Thin-Film Transistors (OTFT). OEDs are building on the interaction between light and matter, mainly semiconductors. In OEDs, light or electromagnetic radiation is absorbed by the semiconductor and its converts into electrical signals and vice versa. The working of LEDs is essentially similar to light and semiconductor interaction [5].

Assume that λ is the wavelength of light, which incident on a semiconductor with band gap E_g. The energy of radiation is given by,

$$E = \frac{hc}{\lambda}$$

Based on the relation between E and E_g, there are two conditions listed below:

$E < E_g$, SC material is transparent, while there could be scattering at the interfaces.

$E > E_g$, SC material is solid and absorb radiation. Usually, this absorption produces electrons in the antibonding and holes in the bonding.

In the direct band gap, SC light absorption occurs for photon energies larger than the energy band gap. In another hand indirect bandgap SC, absorption is smaller, except the photon energy is larger than the direct band gap[6]. The electrons and holes are produced unstable and lose energy to the lattice due to thermal vibration and move to the antibonding and bonding band edge. This can be implicit by occupation probability [(f (E): g (E)] which is maximum close to the band edges.

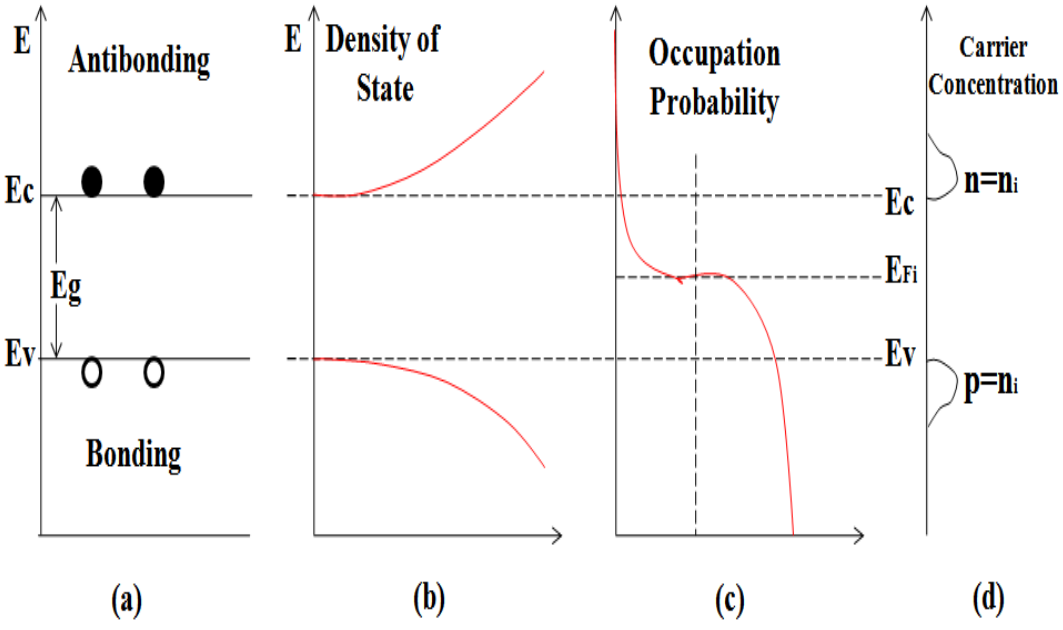

Figure 1: Energy Band Diagram

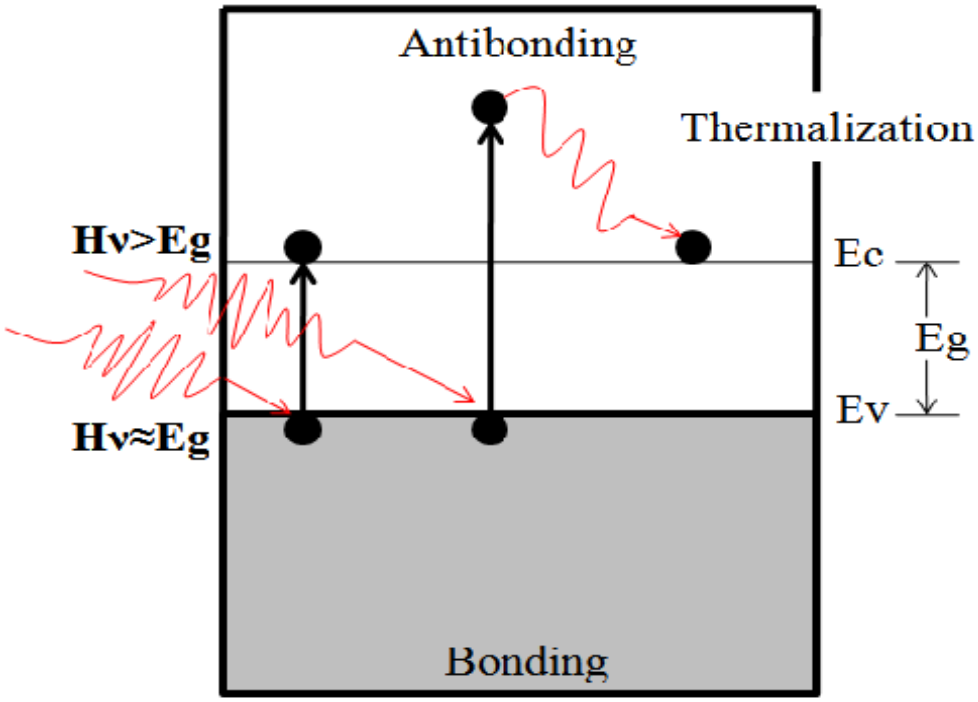

Figure 2: Optical Absorption

If the light energy (E) greater than the energy band gap (E_g), is incident on SC then the overlapped energy ($E-E_g$) is lost due to the lattice vibrations as heat. The optical absorption process is shown in Figure 2. Let I_0 is the intensity of the incident radiation. The intensity is usually mastered in W_m^{-2}. This is related to the photon energy and intensity of radiation is given by

$$I_0 = \Gamma_{ph}(h\nu)$$

1.4.1 OPTICAL SENSORS

An optical sensor is a device or system able to measure, detect and convert light rays into an electronic signal. The intention of an optical sensor is to measure a physical quantity in terms of light and depending on the type of sensors. The optical sensor is used for contact-less detection, counting or positioning of parts. Optical sensor either is internal or external. External sensors gather and transmit a required quantity of light, while the internal sensors are most often used to measure the bends and other small changes in the direction.

TYPES OF OPTICAL SENSOR

There are different types of optical sensors, the most common types which are being used in daily life are listed as below:

- The Photovoltaic cell (solar cell) converts the sum of incident light into voltage.
- Photoconductive devices are used to compute the resistance by changing the sum of incident light into a change in the resistance.
- Phototransistors.

1.4.2 HUMIDITY SENSORS

Selected material is substantial factors to improve the behaviour of the humidity sensor. The material of the sensor should be conductive at the time of reaction with gases or humidity particularly a surface part of semiconductor [10,11,13]. N-type material with relatively little oxygen adsorption sites available is suitable for sensing application to create potential barrier such as zinc oxide. Besides that, the contact added to the semiconductor material also could pick up the humidity sensor performance. Addition process is adding or combining two or more materials such as metal mixed oxide. The advantage of composite sensors are thermally more stable, high electron mobility, have many hetero-contacts between phase and the catalytic of sensing matrix are be able to control [13,14,15].

The formula for calculating sensitivity is:

$$\boldsymbol{Sensitivity} = \frac{\boldsymbol{Change\ in\ Input\ Power}}{\boldsymbol{Change\ in\ \%RH}}$$

Where RH = Relative Humidity (Dimensionless quantity)

The most important specification of humidity sensors are-

- Accuracy
- Repeatability
- Interchangeability
- Long-term stability
- Ability to recover from a reduction

- Resistance to chemical & physical toxin
- Size
- Packing
- Cost-effectiveness.

1.5 STRUCTURAL AND OPTICAL PROPERTIES OF ZINC OXIDE

Zinc oxide is a key technological semiconductor material with wide band gap i.e. 3.37 eV that is suitable for the short wavelength OEDs. The high exciton binding energy i.e. 60 meV of zinc oxide crystals are capable of excitonic emission at room temperature (RT) and ultraviolet (UV) luminescence at room temperature [6]. They require the centre of symmetry in wurtzite, mutual with large electromechanical (EM) coupling, output in well-built piezoelectric and pyroelectric properties and resulting use of zinc oxide in mechanical actuators and piezoelectric sensors. Zinc oxide is a flexible efficient material that has various groups of morphologies such as nanotubes, nanorods, nanowires, nanobelts, nanorings and many more. These zinc oxide nanostructures are easily formed on cheap substrates like glass; hence they give promising potential in the nanotechnology future. Zinc oxide nanoparticles are also attractive for sensors and biomedical applications due to its large surface area. All these applications originated from their basic properties [7].

1.5.1 Basic Properties of Zinc Oxide

Table 1: Shows a set of basic physical parameters of zinc oxide

Properties	Value
Molecular formula	ZnO
Molar mass	81.38 g/mol
Density	5.606 g/cm^3
Appearance	White solid
Band gap	3.3 eV
Odour	Odourless
Crystal structure	Wurtzite

Coordination constant	Tetrahedral
Melting point	1975 ^{o}C
Boling point	2360 ^{o}C
Refractive Index (η_D)	2.0041
Solubility in water	0.0004% (17.8 ^{o}C)
Lattice constant	a=3.25 Å, C=5.2 Å

1.5.2 Crystal Structure

A crystal is a periodic array of atoms. Some of the elements and few compounds are crystalline at low temperature but some of the solid materials in everyday life are not crystalline. The healing of a large number of atoms is simplified if they are arranged in periodic order [3].

The crystal structure is one of the most important forms in material science and engineering as numerous properties of materials depend on their crystal structures. The fundamental of several material characterization techniques such as X-ray diffraction is dependent on crystallography. Understanding the crystals fundamental having ultimate importance. Crystallography is the branch of material science in which crystal structure of crystalline solids is studied. Solids material is classified as given below:

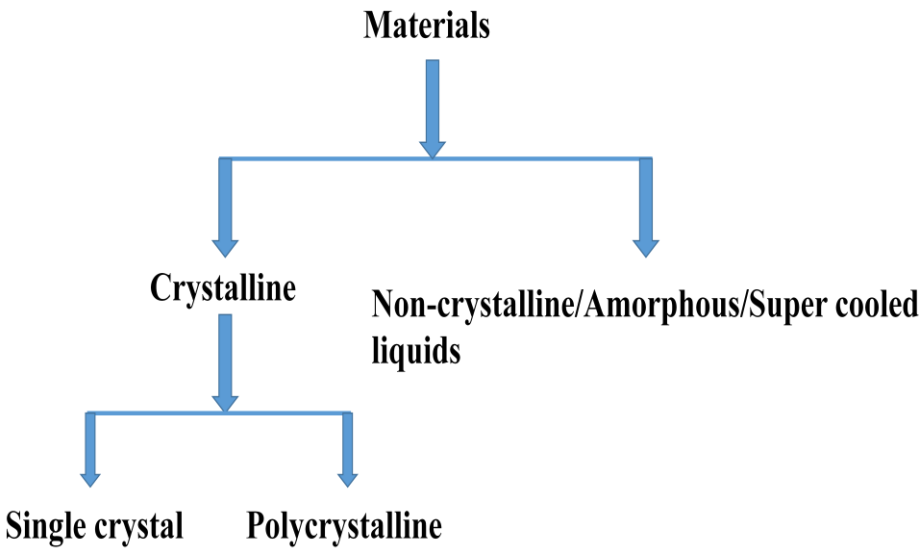

Table 2: Shows the crystal structure of ZnO based on the geometry of unit cell

Crystal system	Lattice parameters	Unit cell Geometry	Bravias Lattice
Hexagonal	a=b≠c, α=β=90°, γ=120°	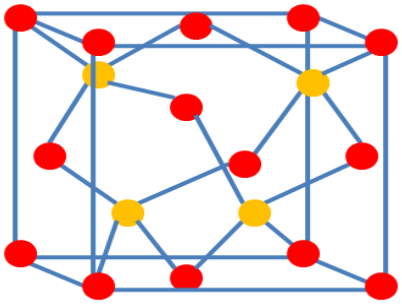	Simple

At ambient temperature and pressure, ZnO crystalline in the tetrahedral wurtzite structure, as shown in Figure 3. This is a hexagonal lattice, belonging to the space group with lattice parameter shown in above Table 2. Usually, it can be considered that there is two type of planes, that is tetrahedral coordinated O^{2-} and Zn^{2+} ions. Another way it can be characterized by two interconnected sublattices of Zn^{2+} and O^{2-} such that each Zn ions is surrounded by a tetrahedral coordination in ZnO will form a non-central symmetric structure with polar symmetry along with hexagonal axis.

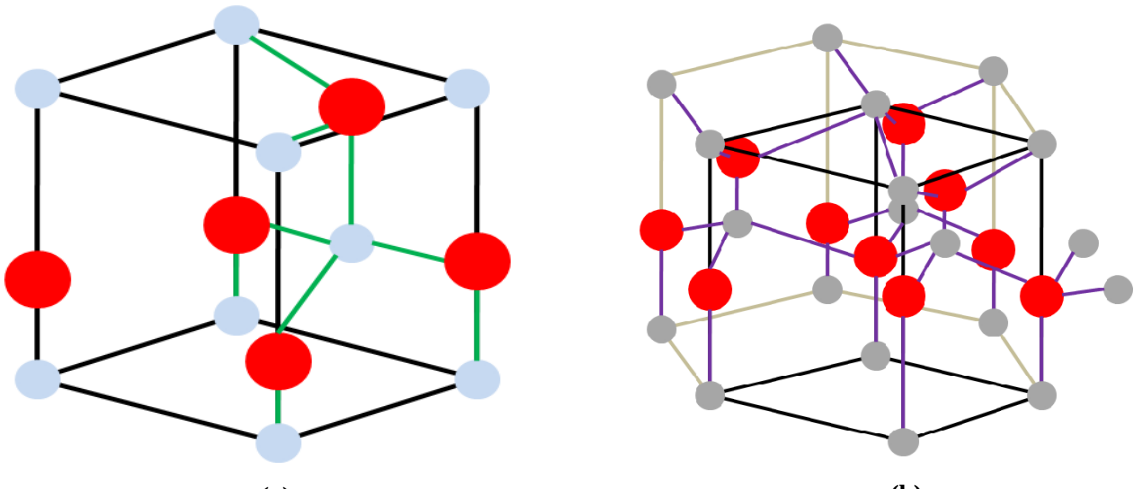

(a) **(b)**

Figure 3: Standard Structure of ZnO, (a) Tetrahedral and (b) Wurtzite Structure

Wurtzite zinc oxide has a hexagonal structure with lattice parameters a = 0.3296 and c = 0.55065 nm. The structure of ZnO can be simply explained as a number of discontinuous planes composed of tetrahedral coordinates. To keep a stable structure, the polar surface generally has facets or exhibits enormous surface reconstructions, but ZnO is exceptions: they are automatically flat, stable and without reconstructions [15,16].

1.5.3 Applications Chart

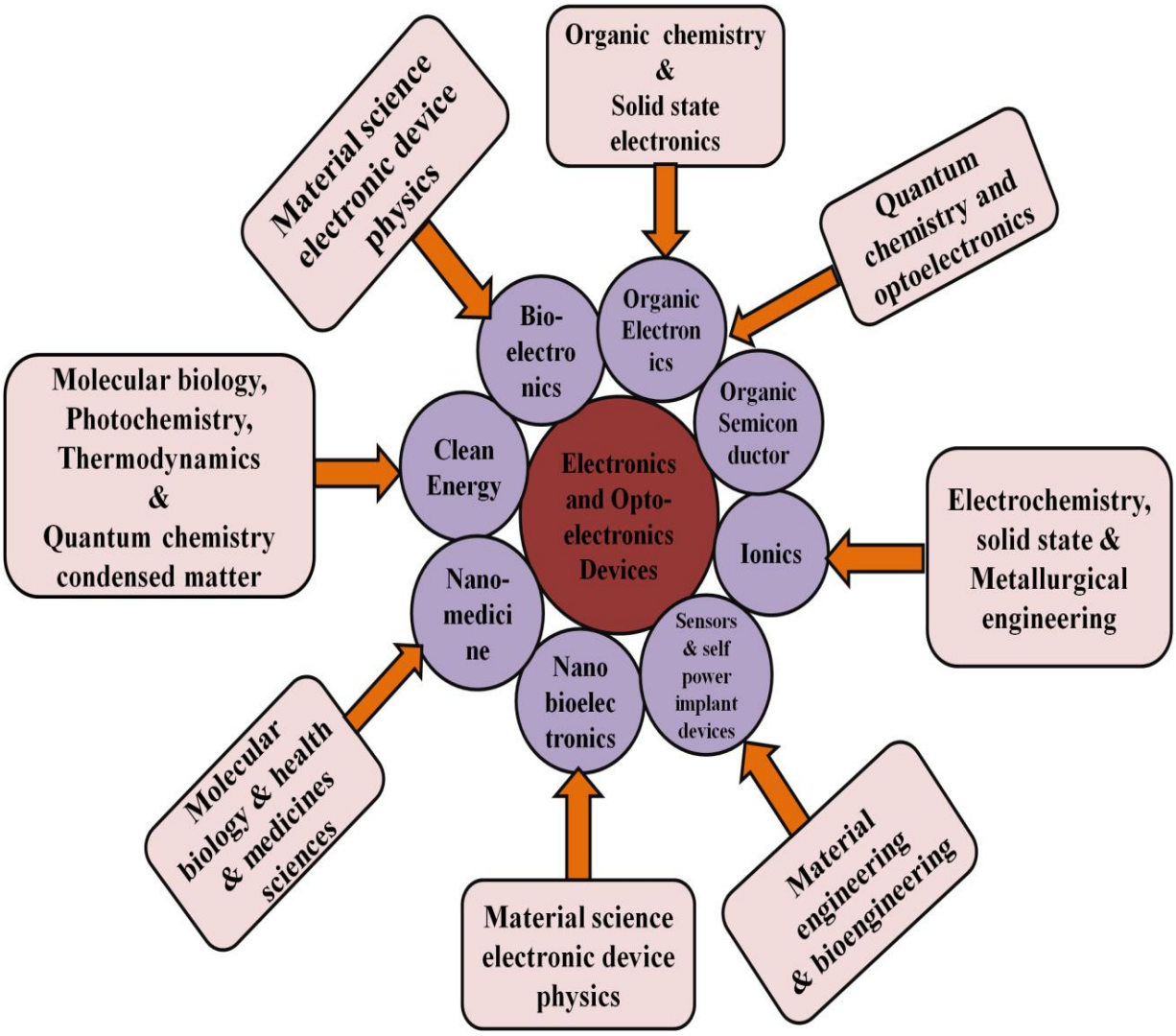

Figure 4: Nano-optoelectronics applications

Nano-optoelectronics is actively researched in the B.B.A.U Lucknow in the department of Electronics and communication, U.I.E.T. Their students are investigating the interaction of light with photonic structures at nanometer dimensions. This has the advantage of expanding bandwidth, low loss and increasing switching speed. The potential applications for this technology are in telecommunication, electronics, optical computing, photon-biology and photon- medicine and sensors. Thermal annealing and packaging processes are also covered, as a key element in a scalable manufacturing process. these include application in the field of electronics (e.g. FET, NMOS, CNT, Schottky diode) and solar energy. It Explores the application areas such as sensing, electronics and solar energy.

CHAPTER

2

2. EXPERIMENTAL TECHNIQUES

2.1 SYNTHESIS PROCESS FLOW CHART

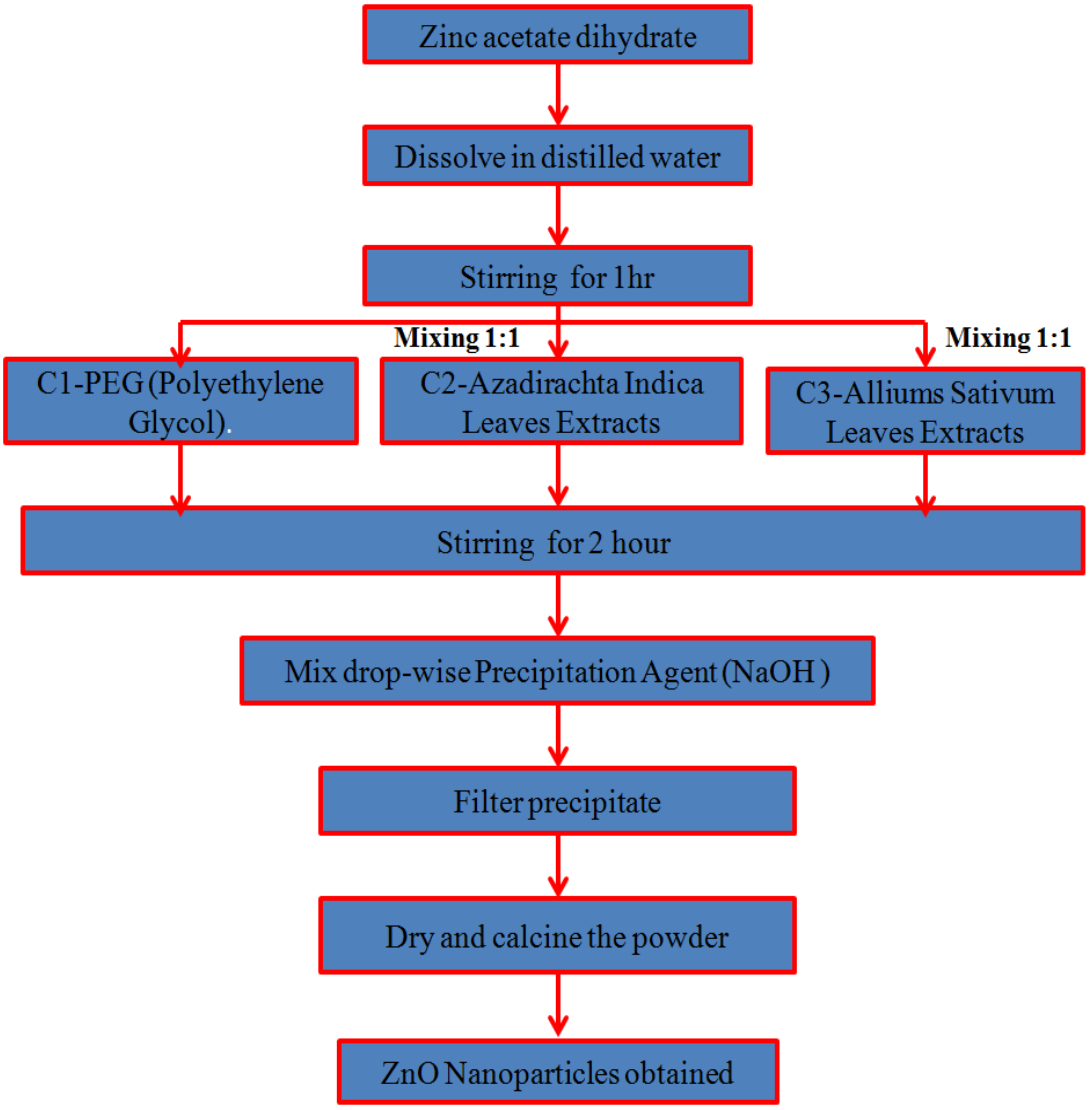

Figure 5: Schematic for the synthesis of ZnO nanoparticles

2.1.1 Synthesis of ZnO Nanoparticles using a capping agent (C-1):

Synthesis of ZnO nanoparticles was successfully done by Chemical Precipitation method. For this 0.1 M of Zinc acetate dihydrate extra pure $(CH_3COO)_2Zn.2H_2O$) was dissolved in distilled water and stirred for an hour. After those 10-12 drops of PEG (Polyethylene Glycol) as a capping agent was added to the solution. PEG was used to reduce the size of the prepared nanoparticles. Then a sufficient amount of NaOH was added to the solution dropwise to maintain the pH 7. The obtained precipitate was dried for 1 hour at 80 ^oC in a microwave oven after that process, calcination of the material was carried out for 4 hours at 400 ^oC in a muffle furnace. Finally, ZnO nanoparticles were obtained in powder form.

Selection of Plant leaves for Green Synthesis: fresh and healthy Azadirachta Indica (**Neem**) & Alliums Sativum (**Garlic**) leaves were collected from B.B.A.U. campus, Lucknow, Uttar Pradesh. The leaves were ensured that they were healthy and uninfected and they were thoroughly washed and rinsed with sterile distilled water and air dried.

2.1.2 Synthesis of ZnO Nanoparticles using Azadirachta Indica (A. I.) leaves extracts (C-2):

Chemical precipitation method is a simple, reliable and eco-friendly. Green synthesis of ZnO nanoparticles was successfully carried out using Chemical precipitation method. For this, initially 0.1 M of Zinc acetate dihydrate extra pure $(CH_3COO)_2Zn.2H_2O$) was dissolved in distilled water and stirred for 1 hour. After stirring, the solution & leaves extract were mixed in the ratio of 1:1 and again stirred for 2 hours. Later NaOH was added to the solution dropwise and the pH was adjusted for precipitate of the solution and the pH was adjusted to 7. The obtained precipitate was dried for 1 hour at 80 ^oC in a microwave oven. After this process, calcination of the material was done for 4 hours at 400 ^oC in a muffle furnace. Finally, ZnO nanoparticles using A. Indica leaves extract were obtained.

2.1.3 Synthesis of ZnO Nanoparticles using Alliums Sativum (A.S.) leaves extracts (C-3):

Green synthesis of ZnO nanoparticles was carried by using alliums sativum leaves extract. Initially, 0.1 M of Zinc acetate dihydrate extra pure $(CH3COO)_2Zn.2H_2O$) was dissolved in distilled water and stirred for 1 hour. After stirring, the precursor & leave extract were mixed in the ratio of 1:1 & stirred again for 2 hours. Later, NaOH was added to the solution dropwise to maintain the pH 7. The obtained precipitate was dried for 1 hour at 80 ^oC in a microwave oven. After this process, calcination of the material was done for 4 hours at 400 ^oC in a muffle furnace. Finally, ZnO nanoparticles using A. Sativum leaves extract were obtained.

2.2 CHARACTERIZATIONS

The morphology of material was investigated using Scanning Electron Microscope (Model: JSM-6490LV, JEOL Japan) at the energy of 30 kV. EDX spectra were obtained for the compositional information of the prepared sample. Fourier Transform Infrared Spectrometer (Nicolet^{TM}6700, Thermo Scientific, U.S.A.) was used to record the absorbance and transmittance spectra by Agilent Technologies. The band gap and absorbance of the material were investigated using the Cary Series UV-Vis Spectrophotometer. The Crystal structure characterization of prepared sample was obtained by the XRD (X' Pert Power). BET analysis was used for obtaining average pore size, average particle size and surface charge. Point zero charge was measured by a pH analyzer.

2.2.1 Scanning Electron Microscopy

For a morphological study, Scanning Electron Microscope, (JSM-6490LV, JEOL, Japan) was used for the energy 30 kV, which gave the black & white colour, 3D images of the sample. SEM is a type of electron microscope which provides a highly magnified image, using the focused scanned electrons beam on the sample. The electrons interact with the atoms of the surface to find the topographical information of the sample. The various emissions obtained for the morphological secondary electron, backscattered electrons and furthermore X-rays. The signals appear from an interaction between the electron beams with the specimens, which differs

in diameter according to different energies of the primary electrons. Each emission has its own importance.

The main characteristics of SEM are-

- Image magnification and resolution are high.
- Quantitative analysis of all elements from carbon upwards can be done.
- Quantitative analysis of solid materials can be done.
- EDX analysis of known or unknown materials can be done.
- Multi-element X-ray mapping and line scans can be done.
- Particle phase, morphology & size can be detected.
- The image can be analysed.

Figure 6: Scanning Electron Microscope, USIC, BBAU

2.2.2 Energy Dispersive X-Ray Spectroscopy

EDX spectroscopy is a quantitative and qualitative micro-analytical X-ray technique that gives information about the chemical composition of a sample for elements with atomic number (Z>3). The intensity or peak possible observed in EDX is proportional to the concentration of the corresponding element in the sample. For shaping element content, the electron beam current must be uniform in the sample and electron channelling should possess the strong diffraction condition.

EDX technique is used for performing chemical analysis in coincidence with SEM. The analytical data are acquired in the form of discrete spectra. The energy of the X-ray transmits hang on the material undergoing to examine. Due to the low-intensity image, it may take maximum hours to generate spectra.

2.2.3 X-ray Diffraction

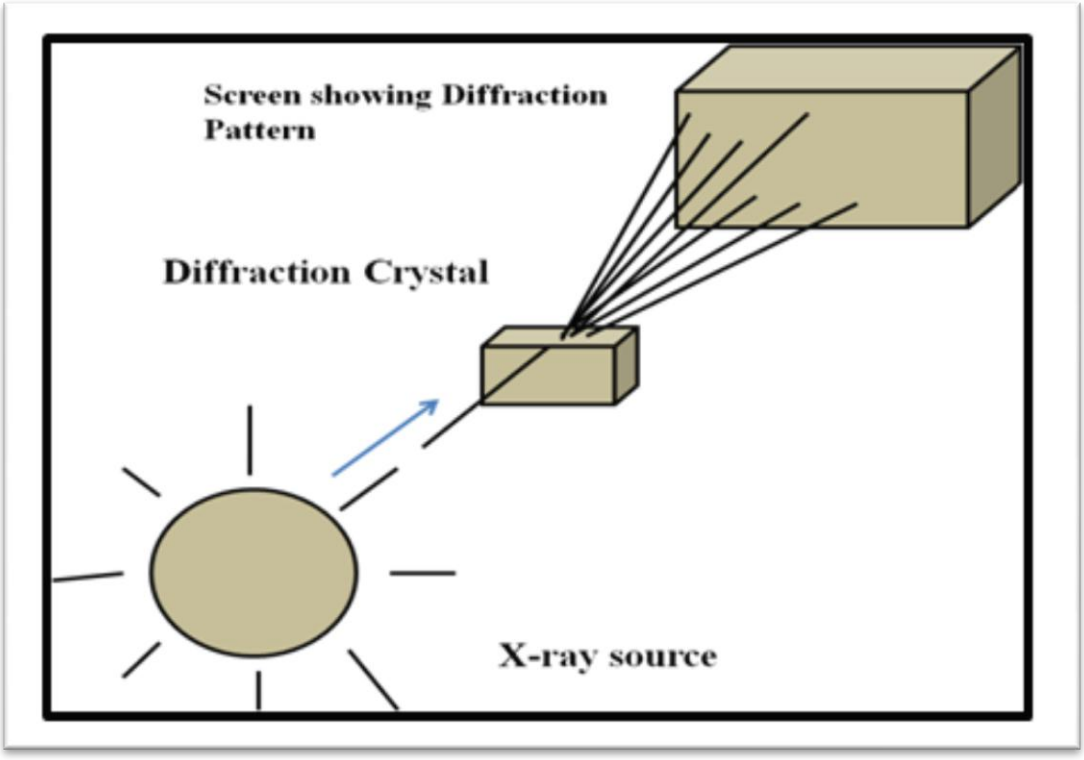

Figure 7 An illustration of the diffraction of X-ray by a crystal

Figure 8: XRD, ACMS, IIT KANPUR

X-ray powder diffraction is a technique to determine ultra small spacing in a material, such as the spacing between atoms in a crystal structure. The X-ray has extremely short wavelength and high energy. PXRD used for phase identification of a crystalline material and capable to offer information about unit dimensions, and it occurs whenever Bragg's law **nλ = 2dsinΘ** is satisfied. Where n is an integer number and λ denotes wavelength. XRD is necessary for material characterization and quality control, which make the use of Debye-Scherrer's formula which is given as below:

$$\mathbf{D} = \frac{\boldsymbol{K\,\lambda}}{\boldsymbol{\beta COS\theta}}$$

Where, D is the mean size of crystallites (nm), K is crystallite shape factor, λ is the X- ray wavelength, β is the full width half maximum (FWHM) in radians of the X-rays diffraction peak and Θ is the Bragg's angle (deg.).

This characterization technique uses X-ray by diffraction on powder samples, where every possible crystalline course is represented equally.

This method gives facility to analyze the unidentified materials and characterizations in the field of metallurgy, mineralogy, archaeology, biology, pharmaceutical and forensic sciences.

OPTICAL CHARACTERISATION

We know that the zinc oxide nanoparticles carry a wide range of application in the field of optoelectronic devices. Optical characterization techniques are listed below, which gives correlated information about optical properties.

- FTIR spectroscopy
- UV-Vis spectroscopy

The optical material is considered for applications in optoelectronics devices like sensor, LED, nanometer-sized thermal sensor detection and biomedical sensing devices.

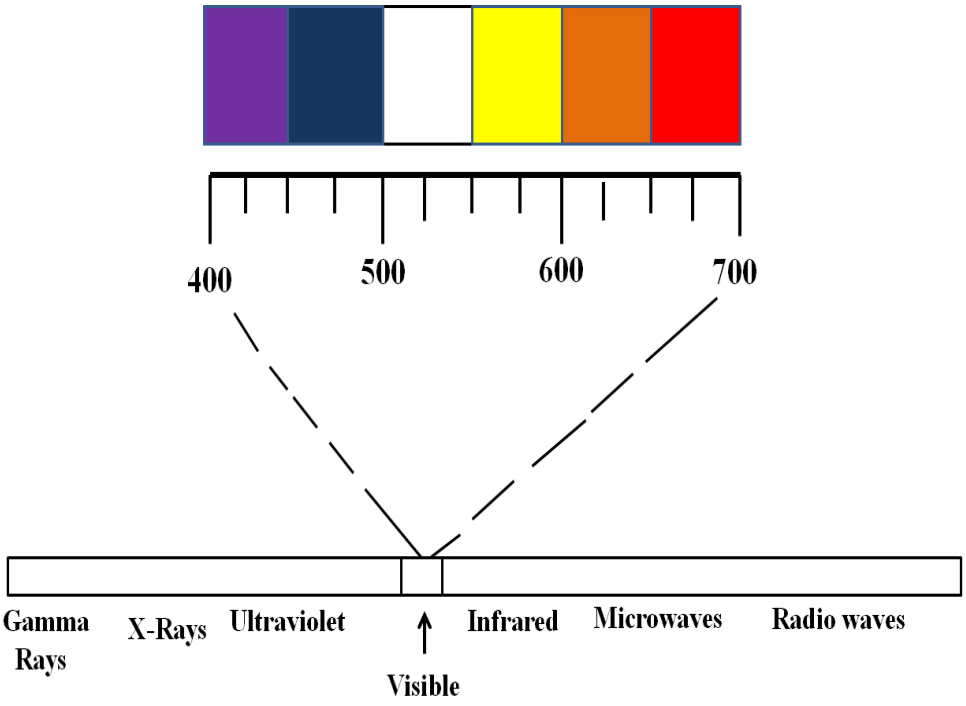

Figure 9: The visible region of the electromagnetic spectrum

2.2.4 Fourier Transform Infrared Spectroscopy

For optical bond analysis, infrared spectroscopy (Nicolet^{TM}6700, Thermo Scientific, U.S.A) is used. Fourier Transform Infrared Spectroscopy (FTIR) is an analytical technique used to classify inorganic, polymer and in several cases, organic materials.

When IR radiation is exposed on a sample, few radiations are absorbed by the sample whereas some are transmitted. The consequential signal at the detector forms a spectrum, which is expressive of a molecular 'fingerprint' of the sample. The effectiveness of infrared spectroscopy is due to the formation of unique peaks for referred to as a different chemical spectral fingerprint. FTIR utilize infrared light to scan samples and observe chemical properties.

2.2.5 UV-Visible Spectrophotometer

Ultraviolet-visible spectroscopy (UV-Vis) refers to absorption spectroscopy in the ultra-violet & visible spectral regions. The spectrometer utilizes light in the visible and adjacent ranges. For quantitative concentration determination of the absorber in the solution of transition metal ions and highly conjugated organic compounds.

Basic Principle

The Beer-Lambert law says that the absorbance of a solution is directly proportional to the concentration of the absorbing sample in the solution and the path length. For a preset path length, UV-Vis spectroscopy can be used to determine the concentration of the absorber in a solution. The absorbance changes depend on concentration. This can be occupied from references or more accurately, determined from a calibration curve.

2.2.6 Brunauer-Emmett-Teller (BET)

Introduction

In the recent years, nanotechnology research has lingering out almost department and into the field of technology, science, IT, medicine, aerospace, and energy etc. the surface to volume ratio is high in case of nanoparticles, however the particle lies in the range of 1 to 100 nm then the different properties are begin occur. For example, commercial grade zinc oxide has the surface range of 2.5-12 m^2/g while zinc oxide nanoparticles surface area can have as high as 54 m^2/g. ZnO nanoparticles have superior UV blocking properties compare to other material.

Overview of BET Theory

The BET was developed by Stephen Brunauer, Paul Emmett and Edward Teller in 1938. The surname letter of each publisher was engaged to name this theory. The BET theory was an extension of the Langmuir theory, developed by Irving Langmuir in 1916. The Langmuir theory related the monolayer adsorption of gas molecules, also called adsorbates, on top of a solid surface to the gas pressure of a medium above the solid surface at a fixed temperature to (1), where Θ is fraction cover of the surface, P is the gas pressure and α is a constant

$$\boldsymbol{\theta = \frac{\alpha P}{1 + \alpha P}}$$

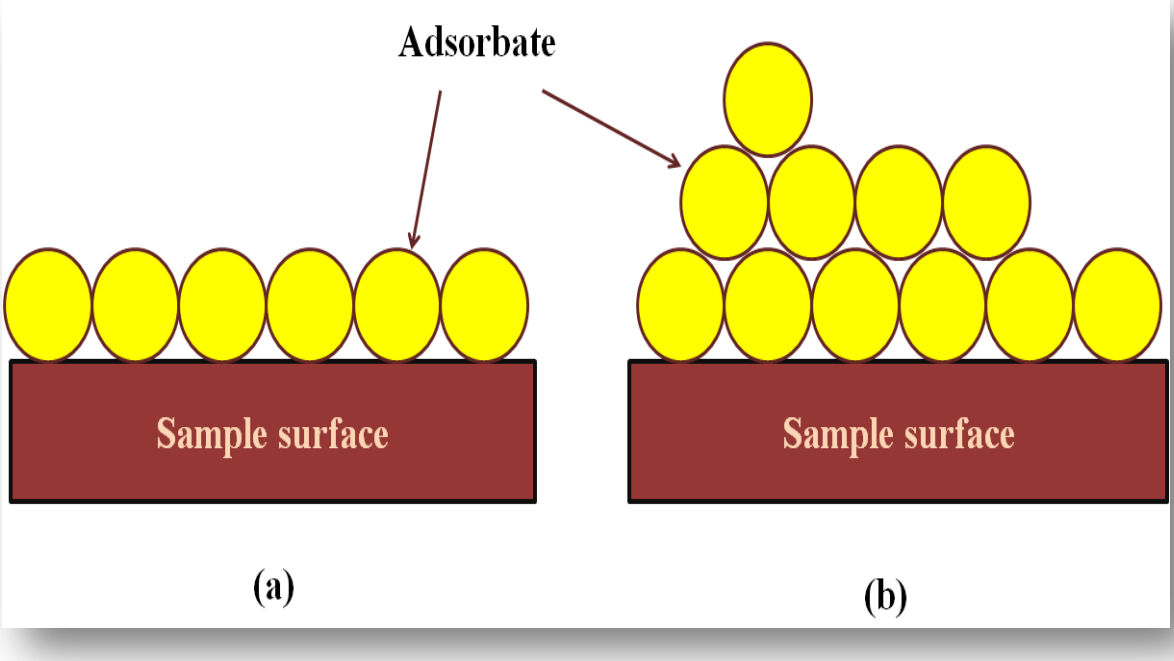

Figure 10: Schematic of the absorption of gas molecules on top of the surface of a sample show (a) the monolayer absorption model said by Langmuir theory and (b) multilayer absorption model said by BET theory

The Langmuir theory is based on the following assumptions:

- All surface sites have the same adsorption energy for the adsorbate, which is frequently used nitrogen or krypton and argon gas. The surface site is defined as the area of the sample where one molecule can absorb against.
- Absorption of the solvent at one site occurs independently of adsorption at nearest sites.
- The motion of adsorbate directly proportional to its concentration.
- Adsorbates from a monolayer.
- Each active site can be filled by only one particle.

BET Working

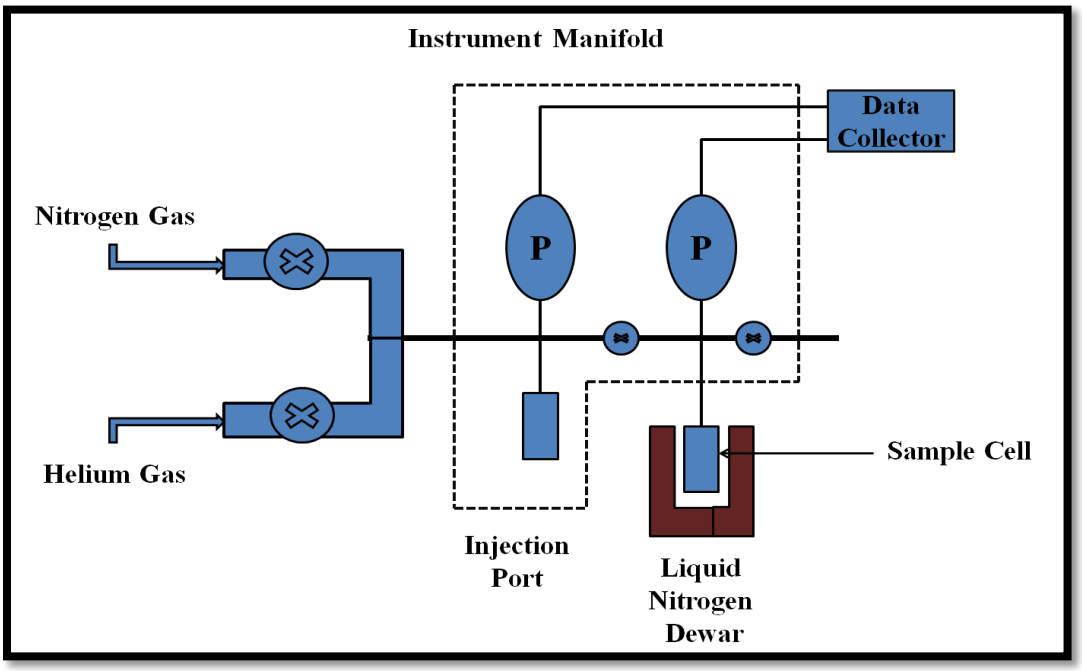

Figure 11: Schematic illustration of BET Instrument

Adsorption is defined as the bond of atoms or molecules of gas to a surface. It should be well-known that adsorption and absorption are not the same; in this, a fluid permeates a liquid or solid. The total gas adsorbed depends on the bare surface are but on the temperature, gas pressure and strength of interaction between the gas and solid. In the BET surface area analysis, nitrogen is frequently used because of its accessibility in high purity and its strong interaction with most of the solids. Because the interaction between gaseous and solids phase is generally weak. The

surface is frozen using liquid N_2 to obtain demonstrable amounts of adsorption. The identified quantity of nitrogen gas is released stepwise into the sample cell. Relative pressure less than atmospheric pressure is achieved by creating a condition of partial vacuum, after the saturation pressure, not mat all adsorption occurs despite any further increase in pressure. Well, precise and accurate layers are formed, the sample is removed from the nitrogen atmosphere and heated to cause the adsorbed nitrogen to be released from the material and quantified. The data collected is displayed in the form of a BET isotherm, which plots the amount of gas absorbed as a function of the relative pressure.

2.2.7 POINT ZERO CHARGE (PZC)

The point zero charge (PZC) is a slightly soluble compound is the pH at which their particles suspended in water have zero charges. The PZC values of slightly soluble hydroxides were compared with the product in the form of its negative logarithm. The cationic completely adsorbed under pH condition where the solution has under negative surface charge i.e. when the pH is above the PZC. Sodium is more strongly adsorbed when the pH-PZC relationship causes the surface charge of ZnO. When the pH-PZC relationship has caused the surface charge of ZnO solution to be positive indicating adsorption of ions. However, greater adsorption occurs when the pH is above PZC.

PZC = (Initial pH of the solution) – (Final pH of the solution)

CHAPTER

3

3. RESULTS AND DISCUSSION

3.1 Table3: Comparison between all three Synthesized ZnO nanoparticles

Parameter	Sample C1	Sample C2	Sample C3
Capping agent	PEG	A.I. leaves extract	A.S. leaves extract
Colour	White	Yellowish	Gray
Odour	Odourless	Pleasant	Nasty
Complexity	Easy	Moderate	Complex
Appearance	Smooth, Creamy	Smooth, Creamy	Smooth, Creamy
pH	8	7	9

3.2 SEM ANALYSIS

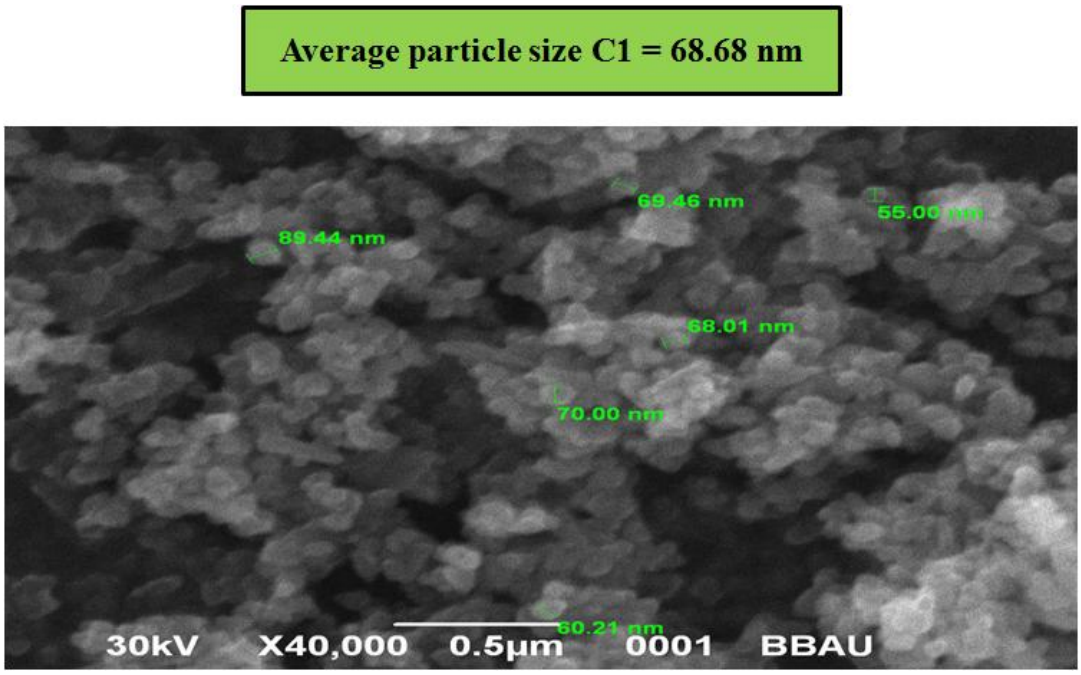

Figure 12: SEM Analysis sample C1, USIC, BBAU

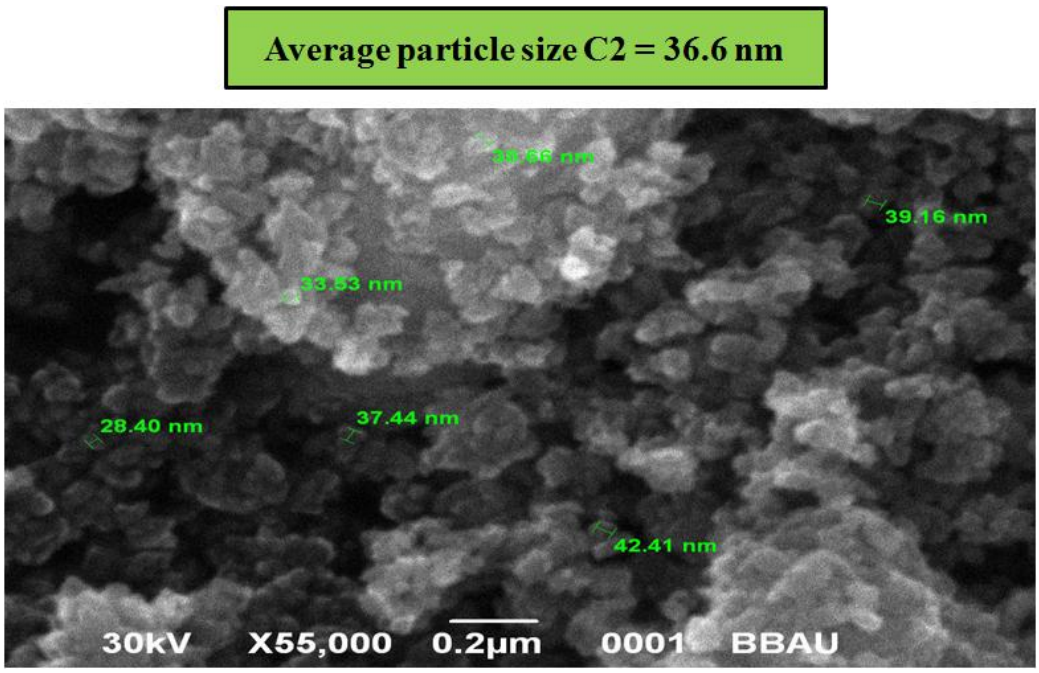

Figure 13: SEM Analysis sample C2, USIC, BBAU

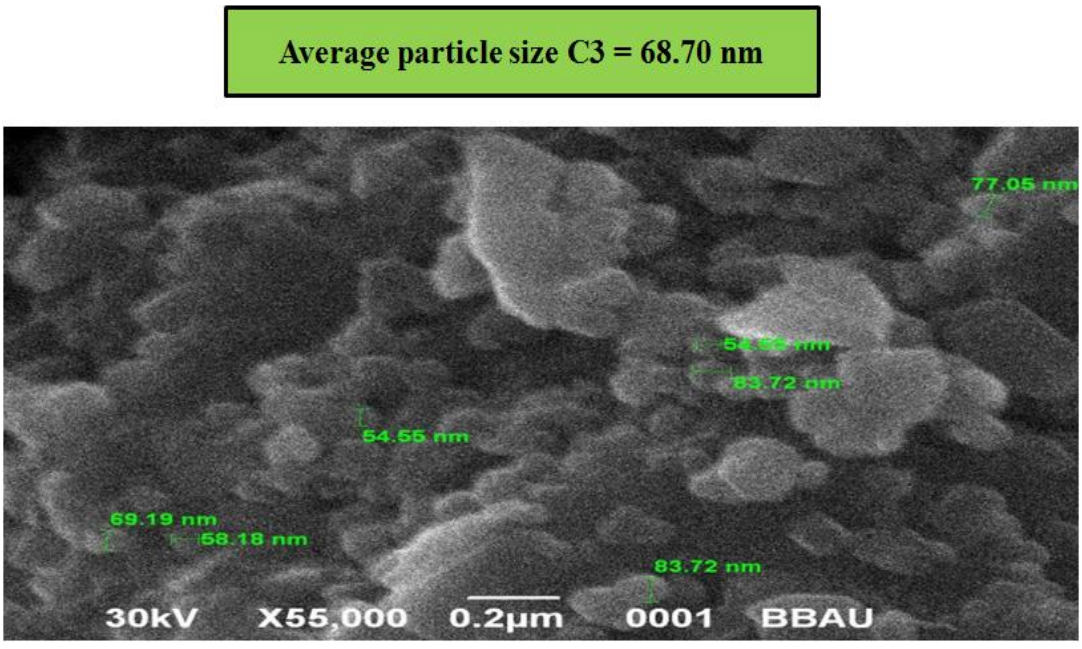

Figure 14: SEM Analysis sample C3, USIC, BBAU

The surface morphology of the prepared sample was not clear due to agglomeration. In the SEM image scanning, the scale was taken 0.5 µm in 40,000 and 0.2 µm in 55,000 times

magnification using power 30 kV of the sample C1 and C2, C3 ZnO nanoparticles shown in Figure 12. The SEM image of the ZnO nanoparticles having Avg. size C1= 68.68 nm, C2 = 36.6 nm and C3 = 68.70 nm and 6, 9 and 11 m length of particles as confirmed by higher magnification image inset of Figure 12. The above SEM image showed a high degree of particles agglomeration is observed. On the other hand, ZnO is polyhedral particles with hexagonal shape of the wurtzite structure observed in PXRD. The best sample C3 average pore size is 51 nm in length.

3.3 EDX ANALYSIS

ELEMENT	WEIGHT%	ATOMIC%
O K	29.96	61.33
Zn K	72.04	38.67
Total	100.00	

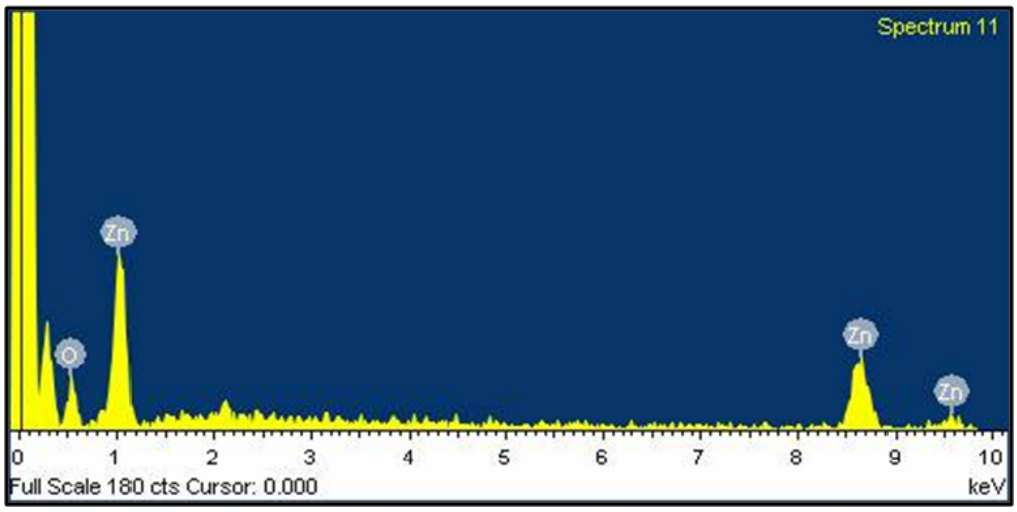

Figure 15: EDX Analysis sample C1, USIC, BBAU

ELEMENT	WEIGHT%	ATOMIC%
O K	33.29	67.10
Zn K	66.71	32.90
Total	100.00	

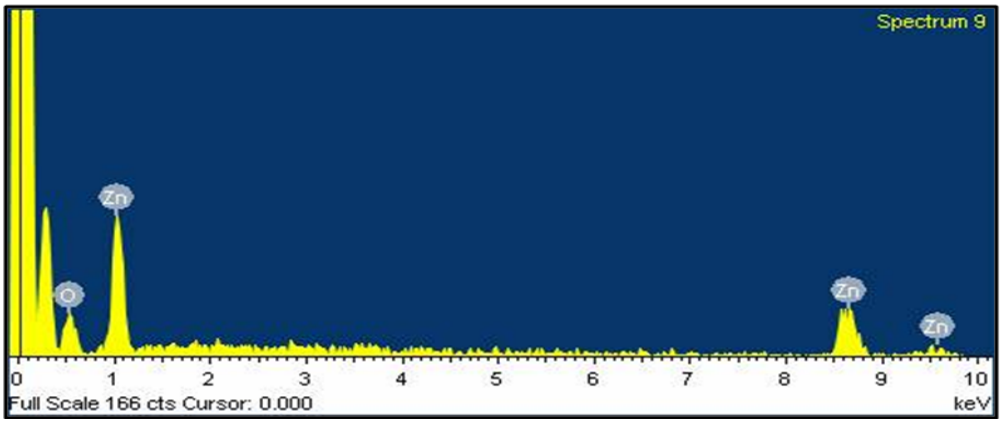

Figure 16: EDX Analysis sample C2, USIC, BBAU

ELEMENT	WEIGHT%	ATOMIC%
O K	15.59	43.01
Zn K	84.41	56.99
Total	100.00	

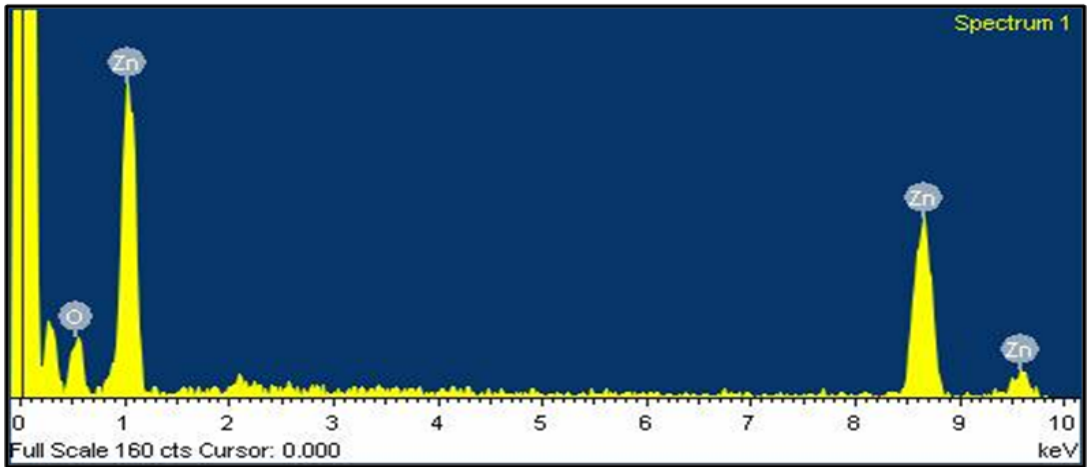

Figure 17: EDX Analysis sample C3, USIC, BBAU

The EDS spectrum of ZnO nanoparticles illustrate peak of zinc and oxygen element, which verify ZnO nanoparticles, prepared mostly free from impurities and it is seen in the limit of EDS Figure 13. Detection lines for the main emission energies for zinc and oxygen and these matches up with a peak in the spectrum, therefore zinc has been discovering correctly. The atomic number and weight percent values of Zn and O shown above Figure13 C1, C2 & C3 respectively. No. of iteration are C1=2, C2=3 and C3= 3 and peak position omitted C1= 2.095 keV.

3.4 FTIR ANALYSIS

FTIR measurements were agreed out to identify the biomolecules for capping agent, a sample of C1, C2 and C3 capably stabilization of the metal nanoparticles synthesized by with leaves extract (C2 & C3) and without leaf extract(C1) ZnO nanoparticles. The FTIR spectrum of zinc oxide (Zn-O) nanoparticles absorbs peak at 456.8, 869.8 and 455.3 cm^{-1}. The corresponding C-O stretching is 873.2, 880.8 and 1364.1 cm^{-1}.

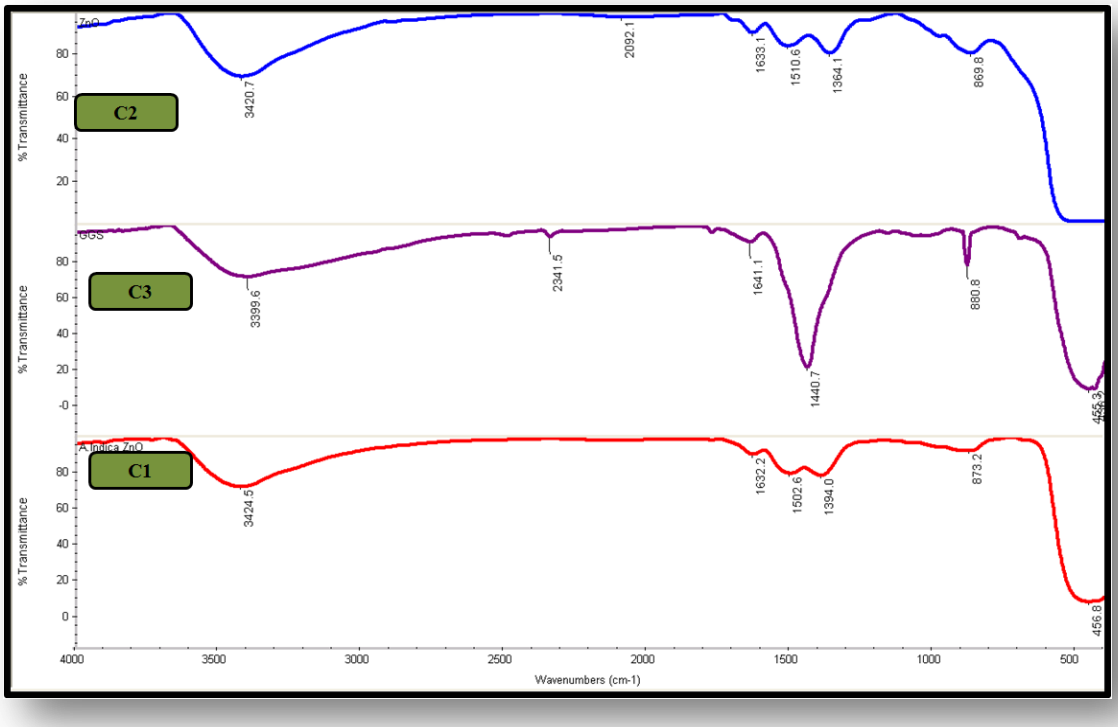

Figure 18: FTIR C1, C2 & C3 Analysis, USIC, BBAU

In this above graph O-H stretching seen along with a C=O peak at 3424.5, 3399.63 and 3420.7 cm^{-1}. Therefore C-F stretching peak point C1=1394, C2=1510.6, C3=1440.7 cm^{-1}. These bands are suggestive of terpenoids group of compounds present in aqueous C1& C3 leaves extract. Some of the major chemical constituents in present in leaves extract (C1 & C3) have been identified trough details by FTIR. A clear O-H stretching peak is observed at 3424.5, 3399.6 and 3420.7 cm^{-1}. FTIR study of dry, finely powder test drug in KB_r Pellet, potassium bromide has the property of being able to be squeezed under very high pressure into a transparent disc- transparent to both Infrared light and visible light. KB_r Pellet confirms the function group.

3.5 UV-Vis SPECTRUM ANALYSIS

UV-Vis absorption spectrum analysis is shown in Figure 15. The ZnO nanoparticles were dissolved in ethanol-water with a concentration of 0.1 wt. % and the solution used to make a thin film for performing UV-measurement. The spectrum reveals the characteristics absorption peak of ZnO at a wavelength of 370 nm, which can be assigned to the intrinsic due to antibacterial properties.

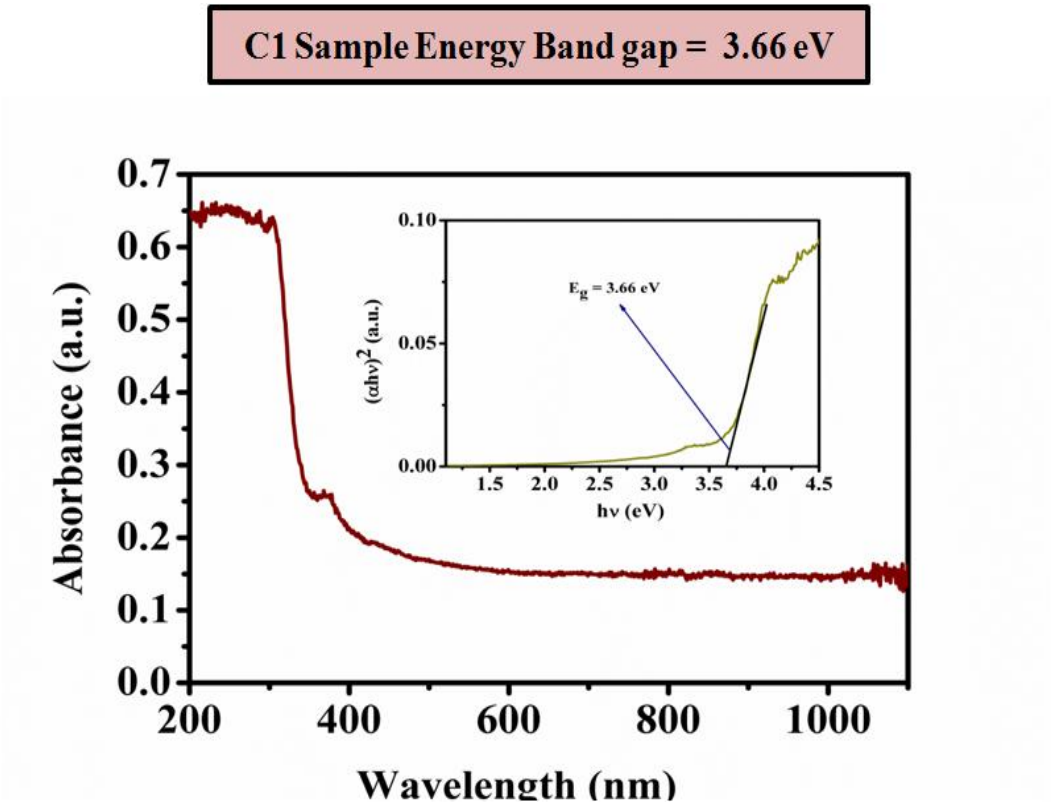

Figure 19: : UV-Vis spectra Analysis of sample C1, BBAU

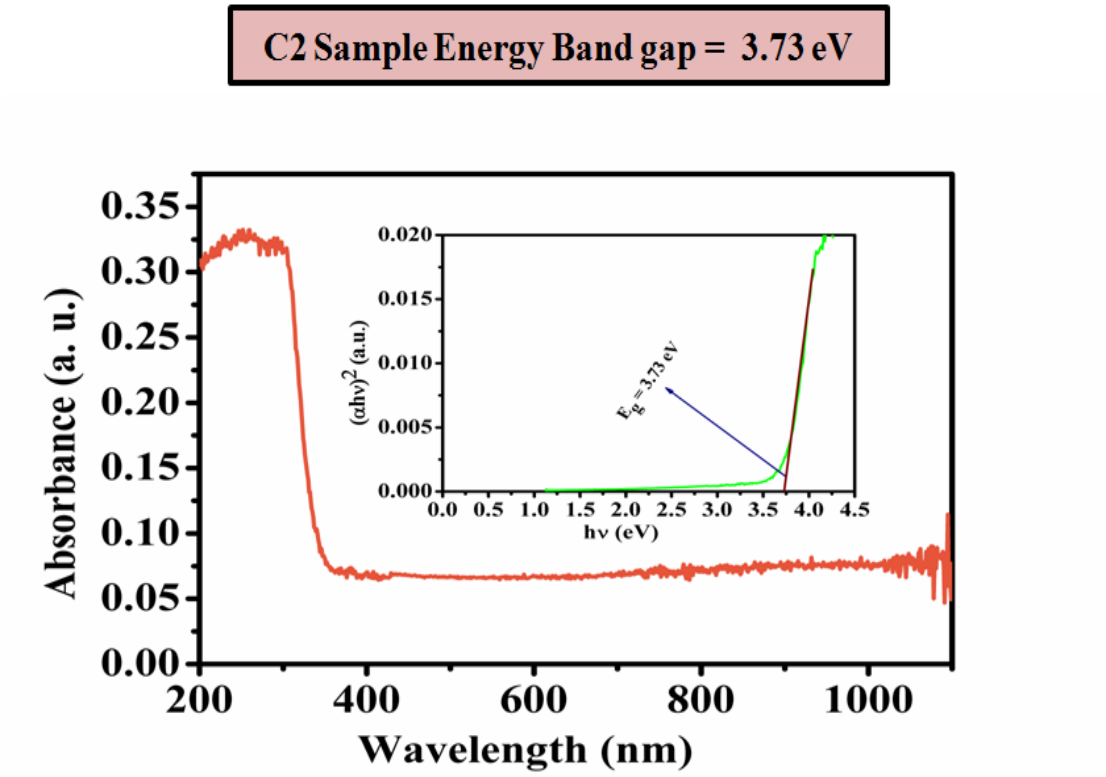

Figure 20: UV-Vis spectra Analysis of sample C2, BBAU

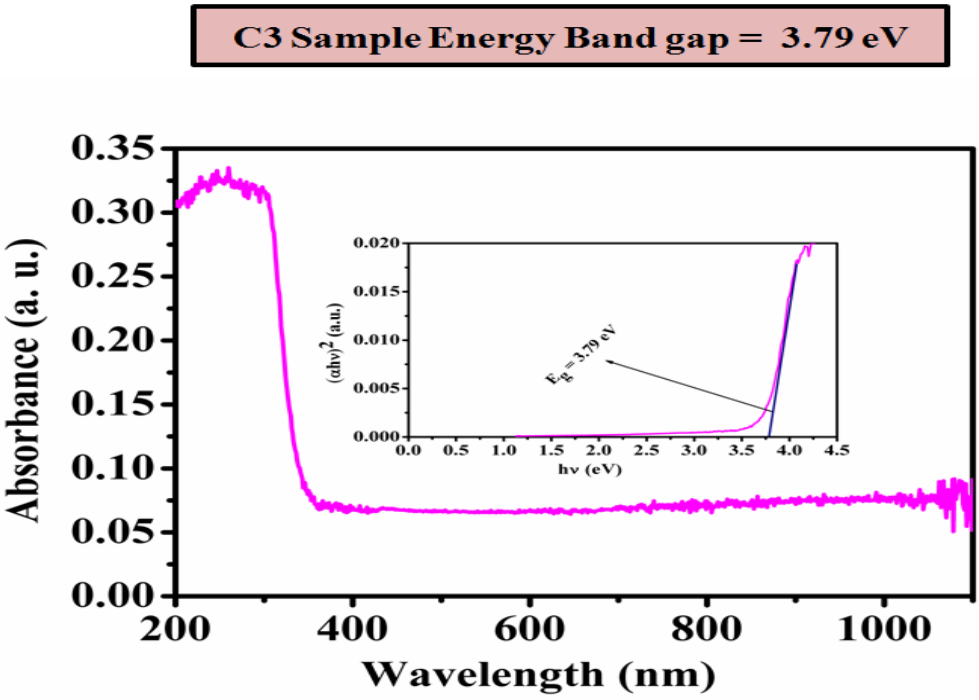

Figure 21: UV-Vis spectra Analysis of sample C3, BBAU

The band gap energy of zinc oxide nanoparticles has been calculated using Tauc's plot presented through the equation.

$$(\alpha h\nu)^2 = B(h\nu - E_g)$$

ZnO nanoparticles are n-type material. For direct bandgap, ZnO nanoparticles band gap found (E_g (C1) = 3.66 eV, E_g (C2) = 3.73 eV & E_g (C3) = 3.79 eV). UV-Visible spectroscopy refers to absorption spectroscopy in the UV-Visible spectral region. It measures the radiation percentage which absorbed at each wavelength. This is done by recording the absorbance and wavelength. This is widely used for the study of the optical band gap of the semiconductor material in Figure 15. The band gap energy of zinc oxide was found to be 3.3 eV.

$$E = \frac{hc}{\lambda}$$

The blue-violet emissions of ZnO are highly popular and they have great potential in light emitting and biological fluorescence labelling applications [11].

3.6 XRD ANALYSIS

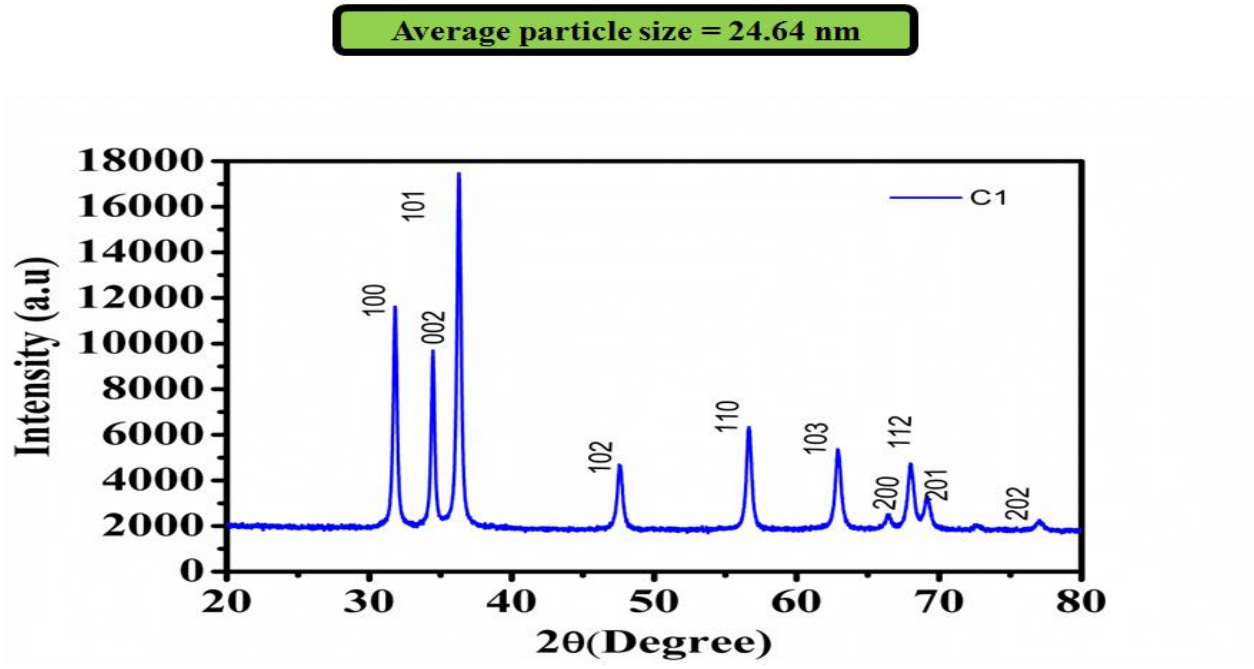

Figure 22: XRD Analysis of sample C1, ACMS, IITK

Average particle size 13.24 nm

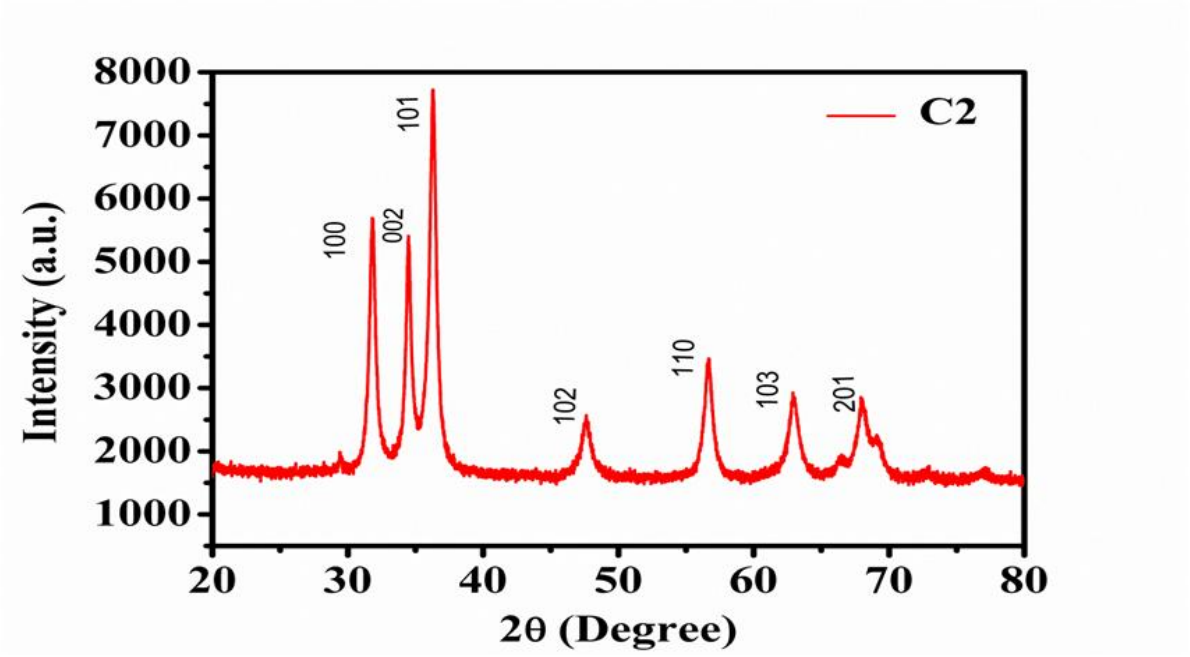

Figure 23: XRD Analysis of sample C2, ACMS, IITK

Average particle size = 10.26 nm

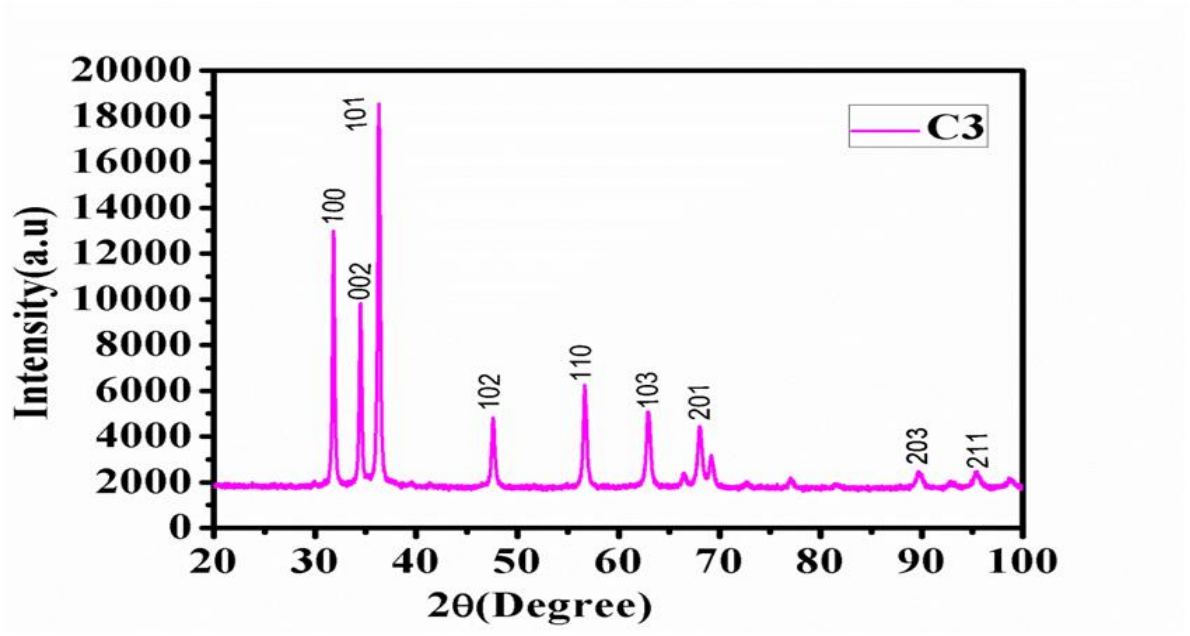

Figure 24: XRD Analysis of sample C3, ACMS, IITK

XRD analysis the crystallite size and structure properties of the ZnO nanoparticles were exposed by using powder X-ray Diffraction. The XRD is approved out with C_uK radiation (λ= 0.154 nm) and 2 theta range from 10° to 100°. The XRD pattern of synthesized ZnO nanoparticles from with or without leaf extract C1, C2 & C3 is shown in Figure 12. The entire peak is restrained ZnO hexagonal phase (wurtzite structure) by comparison with JCPDS card; Reference No. is C1 = 01-074-9940, C2 = 00-003-0888 & C3 = 00-003-0888. The pointed and narrow peaks indicate the product is well crystalline in nature. The full width half maxima (FWHM) of the ZnO (101) line and is the diffraction angle. The mean crystallite size (D) of the nanoparticles was calculated from XRD line boarding measurement using Scherrer's equation. Minimum crystallite size of the powder sample was estimated as 10.26 nm.

3.8 BET ANALYSIS

The specific surface area of a sample was measured using the BET technique (BEL SORP-Mini Japan). This technique includes the pore size distribution (Barrett-Joyner Halenda (BJH)) and Volume analysis. This pore size distribution predicts the dissolution rate, as this rate is proportional to the precise surface area. BET Analysis give precise surface area growth of material by nitrogen multilayer adsorption measured as a function of relative pressure using a fully automated analyzer.

The process of nitrogen adsorption and desorption were shown below. Nitrogen adsorption and desorption theory analysis of the zinc oxide nanoparticles performed at 77 ^{o}k temperature was recorded (Figure 17). The hysteresis that appears as the difference in the two curves at p/p_0 (final and initial pressure). Sample weight = 0.1100 g is due to nitrogen (N_2) reduction (capillary phenomenon) shown by mesoporous material (Fig.17).

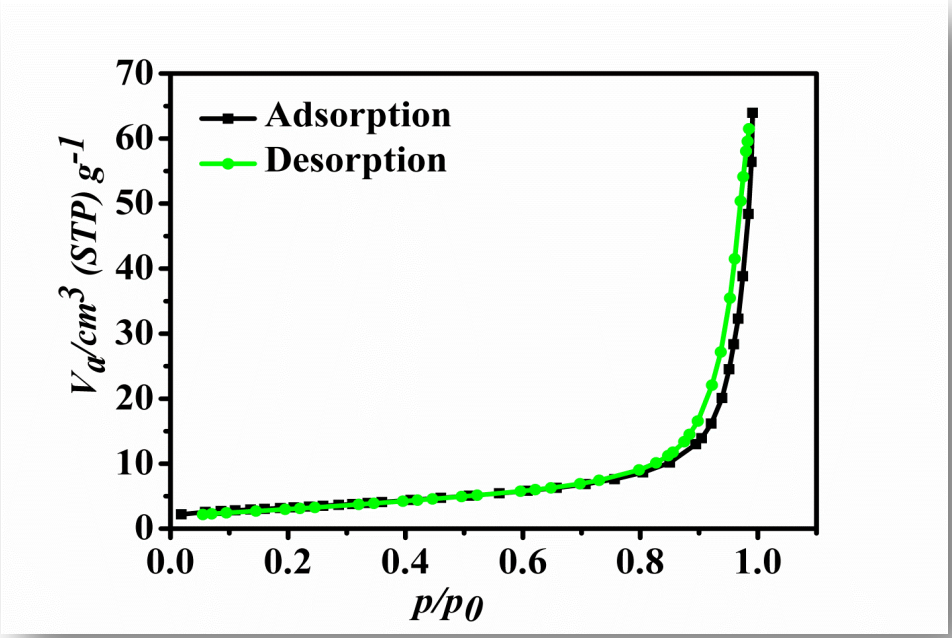

Figure 25: Adsorption & Desorption Analysis, DAC, BBAU

BET size confirms that the zinc oxide nanoparticles carry a precise surface area [S_{BET} = $32.32\ m^2g^{-1}$]. The average pore diameter was found to be **32.513 nm** which is an indication of its mesopores characterization as defined by Dabrowski. According to him, pore diameter ranges as follows: micropores <2 nm, mesopores >2 to 50nm and macropore >50 nm.

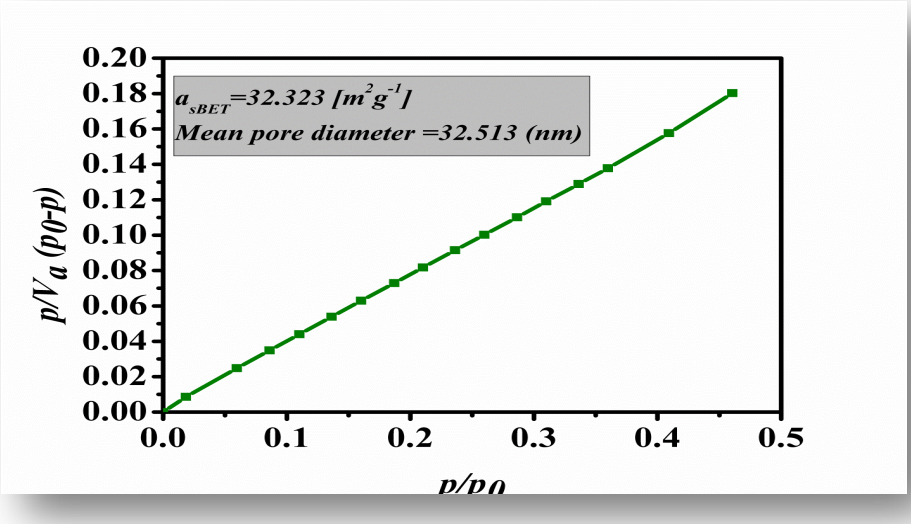

Figure 26: BET Analysis Graph, DAC, BBAU

The BJH calculation was used for plotting a pore size distribution graph, which is shown as BJH plot in Figure 19. It shows the nature of the material.

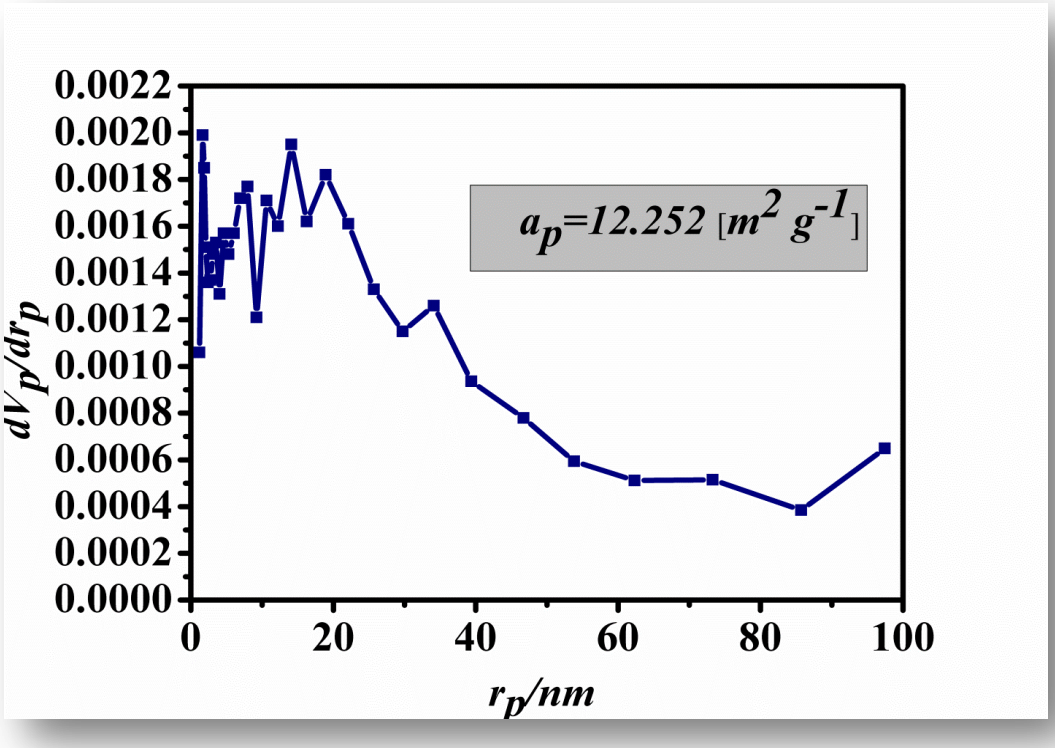

Figure 27: BJH plot, DAC, BBAU

3.8 POINT ZERO CHARGE ANALYSIS

The PZC characteristics of ZnO nanoparticles using alliums sativum leaves extract was determined solid addition method 0.1 M KCL and 0.002 M citramide solution. 40 ml of KCL and citramide solution were taken in a 100 ml stopper conical flask. The initial pH value of the solution was adjusted between 2 to 12 by adding either 0.1 N HCl or 0.1 N NaOH. The total volume of the solution was adjusted to 40 ml by adding 20 ml of KCL and 20 ml of citramide solution. 0.066 gm of ZnO nanoparticles was added to each flask. The suspensions were shaken and allow equilibrating for 24 hours. The PZC value determined by following formula:

The surface potential of the adsorbent may be influenced by the pH value of the co-existing liquid bulk phase. Figure 22 illustrates that pH_{PZC} at ZnO nanoparticles was found to be about **9**

the pH value at which the surface charge is zero, is called point zero charges (PZC). The surface is positively charged at pH < pH_{PZC} and negatevley charge at pH > $pH_{PZC.}$ The surface of the ZnO is **+Ve** charge at Ph > pH_{PZC}, the surface charge is negative [12].

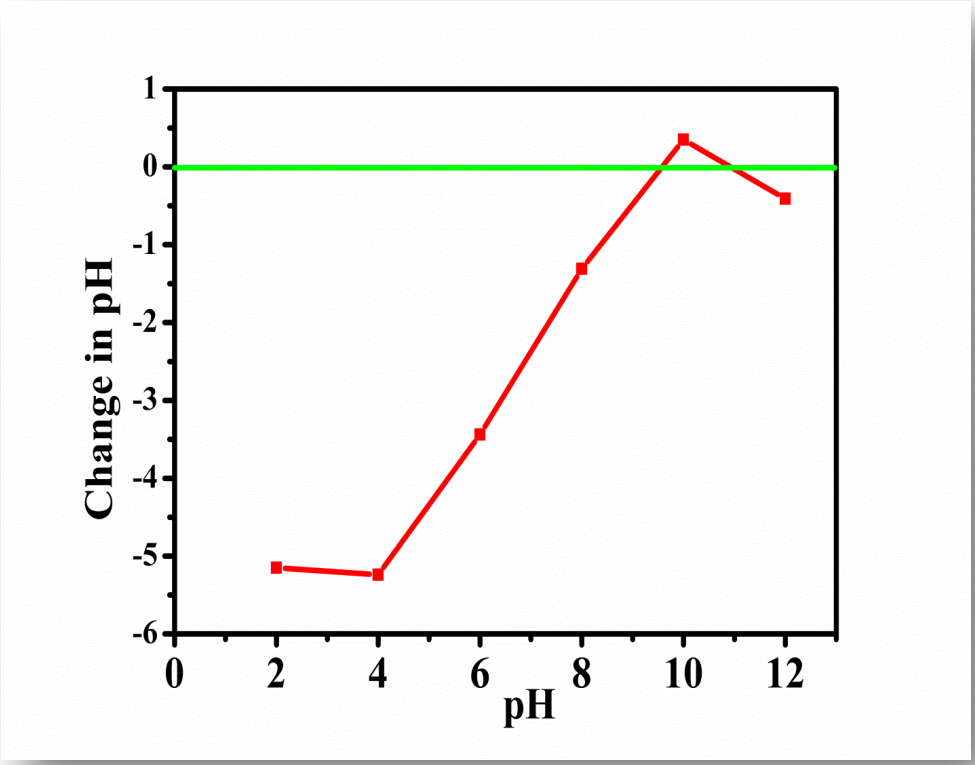

Figure 28: PZC Analysis, DAC, BBAU

CHAPTER 4

4 APPLICATION AND CONCLUSION

4.1 Opto-electronic Humidity Sensor

Monitoring of the humidity is becoming ever more significant for recovering the quality of life and enhancing the industrial progress [19-20]. Humidity sensors based on a variety of working principles have been fabricated to provide the applications. Humidity sensors based on optical methods [21-26] are greatest matched to those situations where remote analysis capability, high sensitivity and density of the device are the criteria for the measurement of humidity levels. Humidity sensors in which the sensing element is a thin film have been broadly calculated [21]. Most of these sensors are based on the variations in the electrical parameters like resistance, conductance or capacitance [27-30]. Very few reports are available in which the optical properties of these films are used to find out the relative humidity [22-27].

4.1.1 Humidity Sensing -Classification & Principles

According to the measurement units, humidity sensors are alienated into two classes: Relative humidity (RH) sensors and Absolute humidity (moisture) sensors. Most humidity sensors are relative humidity sensors and use different sensing principles.

Relative humidity is defined as the ratio of the total moisture content of air to the utmost (saturated) moisture level that the air can hold at a same given temperature and pressure of the vapour. RH is a temperature dependent magnitude and hence it is a relative measurement. The RH measurement is assured as a percentage and determined by the term:

$$\% \, \boldsymbol{RH} = \frac{\boldsymbol{P_v}}{\boldsymbol{P_s}} \times \mathbf{100}$$

where P_v is the actual partial pressure of moisture content in the air and P_s is the saturated pressure of moist air at the same given temperature (both in Bar or Kpa).

4.1.2 Experiment

Figure 21 shows the Experimental setup for optical humidity sensing. A 2 mW He-Ne Laser of wavelength 632 nm was used as a monochromatic light source and a lens combination for diverging the laser beam was used. The prepared film of ZnO nanomaterials (C3) was mounted with the wall of the chamber and a saturated solution of potassium sulphate (K_2SO_4) was placed inside the chamber for increasing humidity continuously from 10-95 % RH inside the chamber. A hygrometer (Huger, Germany) was used for recording the variations in moisture levels. The transmitted laser light was focussed on Detector and variations in output power was recorded. For decreasing the humidity inside the humidity chamber from 95 to 10 %RH, a saturated solution of potassium hydroxide (KOH) was used.

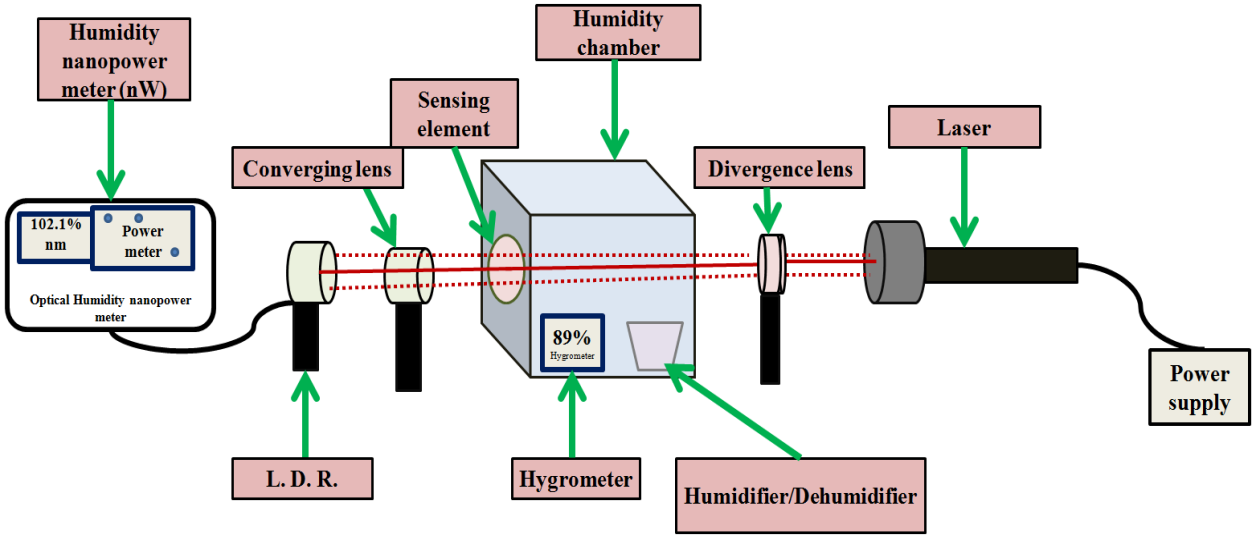

Figure 29: Optoelectronics Humidity sensing Setup

Table 4: The following table is shown important parameters of ZnO thin film based Optoelectronic Humidity Sensing:

Sensed Parameter	**Remarks**
Measured Parameters	% RH
RH change	10 % to 95 %

RH accuracy	± 1 % to ± 3 %
Interchangeability	Poor
Linearity	Moderate
Rise time	3 Min to 5 Min
Temperature	35 ^{o}C
Long-term stability	± 3 % PH/ yr
Hysteresis	< 2 % H
Sensitivity	9.93 µW / %RH

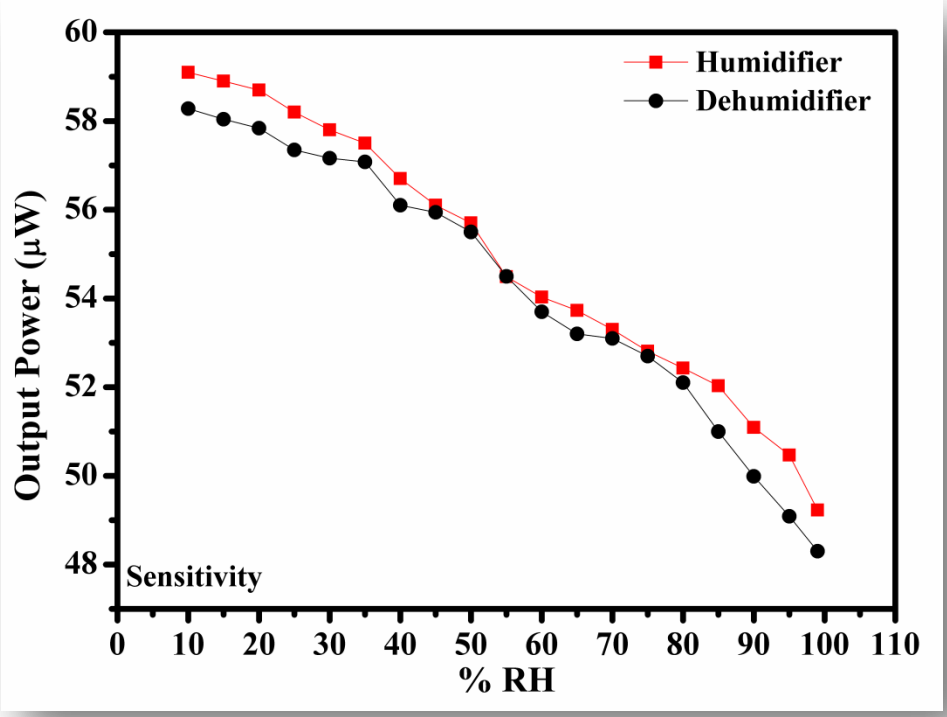

Figure 30: Variation of Output Power Verses %RH

Figure 30 shows the variation in output power for the thin film of ZnO nanoparticles with the relative humidity (%RH) in the range of 10-95% at 35 ^{o}C. It can be observed from the figure that as %RH increases, O/P power decreases. The plot of power versus RH from 10% to 95 %,

illustrates good humidity sensing along with the reproducibility. The measurement of power – RH characteristics was repeated for every 4 days in a month. Only slight deviation in resistance at each humidity region was observed over time after ageing, proving good stability and durability of the ZnO nanoparticles based humidity sensor.

- 10 % to 30 % = Lower Relative Humidity,
- 30 % to 70 % =Intermediate Relative Humidity
- 70 % to 99 % = Higher Relative Humidity
    - Sensitivity Lower Region **($S_{L)}$ = 1.07 µW/%RH**
    - Sensitivity Intermediate Region **(S_{IM}) = 4.06 µW/%RH**
    - Sensitivity Higher Region **(S_H) = 4.8 µW/%RH**

Total Sensitivity $_{(Hum)}$ = 9.93 µW / %RH

Total Sensitivity $_{(Dehum)}$ = 9.89 µW / %RH

Table5: Overall Analysis results shown in the following table-

Characterization	**Sample C1**	**Sample C2**	**Sample C3**
SEM, avg. Particle size	68.68 nm	36.6 nm	68.70 nm
Energy Band gap	3.66 eV	3.73 eV	3.79 eV
XRD, Avg. particle size	24.64 nm	13.24 nm	10.26 nm (Best)
Structure	Hexagonal	Hexagonal	Hexagonal
BET, Surface area	-	-	S_{BET} = 32.32 $[m^2g^{-1}]$
BET, Mean pore diameter	-	-	32.513 nm
BET, Avg. Particle size	-	-	a_p = 12.252 $[m^2g^{-1}]$
SENSITIVITY	-	-	9.93 µW / %RH

4.2 CONCLUSION

With or without leaves extract hexagonal structured ZnO nanoparticles were successfully prepared. The sensing characteristics towards humidity indicated that green synthesized ZnO structure gives the highest sensitivity compare to ZnO nanoparticles. It was due to the distribution of porosity on the surface of ZnO structure and large surface specific area for adsorption and desorption process. Besides, the stability and reproducibility performance of ZnO structure carry out that it's was suitable for humidity sensor application. The resistance decreases exponentially with the increasing RH. The adsorption and desorption of moisture rates and Gibbs free energy kinetic parameters were determined by using a dynamic Langmuir model. The values of adsorption and desorption rates were calculated as 3453.6 m^{-1} s^{-1} and 0.0147s^{-1}, respectively. The Gibbs free energy for adsorption cycles was found to be as - 30.64 kJ / mol. Thus, results show that the ZnO nanoparticles are very sensitive to relative humidity changes and give reproducible adsorption and desorption kinetic behavior for both short and long time periods. The XRD results reveal that the formation of a hexagonal phase that has a predominant (002) plane of ZnO nanoparticles with an average crystallite size of 24.64 nm (C1), 13.24 nm (C2) and 10.26 nm (C3). SEM revealed the morphology of the materials and EDX confirmed the material presence. FTIR analysis confirmed the formation of ZnO nanoparticles bonds. UV-Vis. Spectra analysis gave the Band gap of the ZnO nanoparticles as EgC_1 = 3.66 eV, EgC_2 = 3.73 eV & EgC_3= 3.79 eV. BET analysis confirmed a highly mesoporous structure of the ZnO nanoparticles. Maximum pore diameter was observed as 32.513 nm. The total process was eco-friendly, cost effective and easy to operate. For the future, Green synthesized ZnO nanoparticles exhibits huge possibilities in sensing devices.

REFERENCES

[1] S. Logothetidis (ed), "Nanostructured materials and their applications", Nanoscience and Technology, Springer- Verlag Berlin Heidelberg 2012.

[2] M.F. Fakoya, S.N. Shah, "Emergence of nanotechnology in the oil and gas industry: Emphasis on application of silica nanoparticles", Petroleum 3 (2017) 391-405.

[3] J.D. Miller, " A Handbook on nanophysics".

[4] S. Mokkspati, C. Jagdish, "III-V compound SC for optoelectronics devices". Elsevier April 2009 Volume 12 | number 4 22-32.

[5] C. Musumeci, A Liscio, V. Palermo, P. Samori, "Electronic characterization of supermolecular materials at the nanoscale by Conducting Atomic Force and Kelvin Probe Force microscopic", Elsevier Volume 17, Number 10 December 2014.

[6] P. Zu, Z.K. Tang, G.K.L. Wong, M. Kawasaki, A. Ohtomo, H. Koinuma, Y. Segawa, "Ultraviolet spontaneous and stimulated emission from ZnO microcrystallite thin film at room temperature", Solid State Communications 103 (1997) 459-463.

[7] L. Vayssieres, K. Keis, A. Hagfeldt, S.E. Linquist, "Three-Dimensional array of Highly oriented crystalline ZnO microtubes", Chemistry of Materials 13 (2001) 4395-4398.

[8] J. Kenkel, "Analytical chemistry CRC".

[9] R. Krishnaveni, S. Thambidurai, "An Industrial method of cotton fabric finishing with chitosan ZnO composite for antibacterial and thermal stability", Ind. Crops Prod. 47 (2013) 160-167.

[10] Korotcwnkov G 2007 Metal oxide for the solid-state gas sensor: what determines our choice? Material Science and Engineering: B139 1-23.

[11] C. Wang, L. Yin, L. Zhang, D. Xiang and R. Gao, 2010 "Metal oxide gas sensor: Sensitivity and influencing factors Sensors", 2010 10 2088-106.

[12] K. Singh, S.K. Verma and R. Bharose, "Powdered activated mustard cake (PAMC): Synthesis, characterization and its use for aqueous phase adsorption of phenolics", J.Indian Chem. Soc., Vol.91, March 2014, pp.483-496.

[13] N. Singh, A. Ponzoni, E. Comini and P.S. Lee, "Chemical sensing investigations on ZnO" Sensors and Actuators B: Chemical 171-172 244-8.

[14] J Yu and G.M. Choi, "Electrical and CO gas-sensing properties of ZnO hetero-contact", Sensors and Actuators B: Chemical, 1999 61 59-67.

[15] Haeng Yu J and Man Choi G, "Electrical and CO gas sensing properties of ZnO-SnO_2 composites", Sensors and Actuators B: Chemical, 1998 52 251-6.

[16] O Dulub , LA Boatner and U Diebold 2002 Surf. Sci. 519 201.

[17] Meyer B and Marx D 2003 Phys. Rev. B **67** 035403.

[18] B. C. Yadav, S. Sikarwar "Optoelectronic Humidity Sensor: A review", Sensors and Actuators A233 (2015) 54-70.

[19] H. Farahani, R. Wagiran and M.N. Hamidon, "Humidity Sensors Principle, Mechanism, and Fabrication Technologies: A Comprehensive Review", Sensors 2014, 14,7881-7939.

[20] B.M. Kulwicki, "Humidity sensor", Journal of the American Ceramic Society 74(4), 1991, pp. 697-708.

[21] C. Zhi and L. Chi, "Humidity sensor: A review of materials and mechanisms", Sensor Letters 3(4), 2005, pp. 274-295.

[22] D. Eisenberg and W. Kaufmanns, "The Structure and Properties of Water", Oxford University Press, 1969.

[23] K. Ogawa, S. Tsuchiya, H. Kawakami, T. Tsutsui, "Humidity- sensing the effect of optical fibers with microporous SiO_2 cladding", Electronics Letter 24(1), 1988,pp. 42-43.

[24] A. Kharaz, B.E. Jones, "Adistributed Optical- fiber sensing system for multi-point humidity measurement", Sensor and Actuators A: Physical, 47(1-3), 1995, pp. 491-493.

[25] L.M Bali, B.C. Yadav, G.C. Dubey, R.K. Srivastava, A. Srivastava, R.N. Singh, "Optical humidity sensor", 7th National Seminar on Physics & Technology of Sensors, Pune, India 2007, pp.C.35.1-C.35.6.

[26] B.C. Yadav, N.K. Pandey, A.K. Srivastava, P. Sharma, "Optical humidity sensors based on titania films fabricated by sol-gel and thermal evaporation methods", Measurement Science and Technology 18(1), 2007, pp. 260-264.

[27] S.K. Shukla, G.K. Parashar, A.P. Misra, P. Misra, B.C. Yadav, R.K. Shukla, L.M. Bali, G.C. Dubey, "Nano-like magnesium oxide film and its signification in optical fiber humidity sensor", Sensor and Actuators B: Chemical 98(1), 2004, pp. 5-11.